NASA/TM—2009-215611 AIAA–2008–4527

Performance Characteristics of the NEXT Long-Duration Test After 16,550 h and 337 kg of Xenon Processed

Daniel A. Herman
ASRC Aerospace Corporation, Cleveland, Ohio

George C. Soulas and Michael J. Patterson
Glenn Research Center, Cleveland, Ohio

May 2009

NASA STI Program . . . in Profile

Since its founding, NASA has been dedicated to the advancement of aeronautics and space science. The NASA Scientific and Technical Information (STI) program plays a key part in helping NASA maintain this important role.

The NASA STI Program operates under the auspices of the Agency Chief Information Officer. It collects, organizes, provides for archiving, and disseminates NASA's STI. The NASA STI program provides access to the NASA Aeronautics and Space Database and its public interface, the NASA Technical Reports Server, thus providing one of the largest collections of aeronautical and space science STI in the world. Results are published in both non-NASA channels and by NASA in the NASA STI Report Series, which includes the following report types:

- TECHNICAL PUBLICATION. Reports of completed research or a major significant phase of research that present the results of NASA programs and include extensive data or theoretical analysis. Includes compilations of significant scientific and technical data and information deemed to be of continuing reference value. NASA counterpart of peer-reviewed formal professional papers but has less stringent limitations on manuscript length and extent of graphic presentations.

- TECHNICAL MEMORANDUM. Scientific and technical findings that are preliminary or of specialized interest, e.g., quick release reports, working papers, and bibliographies that contain minimal annotation. Does not contain extensive analysis.

- CONTRACTOR REPORT. Scientific and technical findings by NASA-sponsored contractors and grantees.

- CONFERENCE PUBLICATION. Collected papers from scientific and technical conferences, symposia, seminars, or other meetings sponsored or cosponsored by NASA.

- SPECIAL PUBLICATION. Scientific, technical, or historical information from NASA programs, projects, and missions, often concerned with subjects having substantial public interest.

- TECHNICAL TRANSLATION. English-language translations of foreign scientific and technical material pertinent to NASA's mission.

Specialized services also include creating custom thesauri, building customized databases, organizing and publishing research results.

For more information about the NASA STI program, see the following:

- Access the NASA STI program home page at *http://www.sti.nasa.gov*

- E-mail your question via the Internet to *help@sti.nasa.gov*

- Fax your question to the NASA STI Help Desk at 301–621–0134

- Telephone the NASA STI Help Desk at 301–621–0390

- Write to:
  NASA Center for AeroSpace Information (CASI)
  7115 Standard Drive
  Hanover, MD 21076–1320

NASA/TM—2009-215611 AIAA–2008–4527

Performance Characteristics of the NEXT Long-Duration Test After 16,550 h and 337 kg of Xenon Processed

Daniel A. Herman
ASRC Aerospace Corporation, Cleveland, Ohio

George C. Soulas and Michael J. Patterson
Glenn Research Center, Cleveland, Ohio

Prepared for the
44th Joint Propulsion Conference and Exhibit
cosponsored by the AIAA, ASME, SAE, and ASEE
Hartford, Connecticut, July 21–23, 2008

National Aeronautics and
Space Administration

Glenn Research Center
Cleveland, Ohio 44135

May 2009

This report contains preliminary findings,
subject to revision as analysis proceeds.

Level of Review: This material has been technically reviewed by technical management.

Available from

NASA Center for Aerospace Information
7115 Standard Drive
Hanover, MD 21076–1320

National Technical Information Service
5285 Port Royal Road
Springfield, VA 22161

Available electronically at http://gltrs.grc.nasa.gov

Performance Characteristics of the NEXT Long-Duration Test After 16,550 h and 337 kg of Xenon Processed

Daniel A. Herman
ASRC Aerospace Corporation
Cleveland, Ohio 44135

George C. Soulas and Michael J. Patterson
National Aeronautics and Space Administration
Glenn Research Center
Cleveland, Ohio 44135

Abstract

The NASA's Evolutionary Xenon Thruster (NEXT) program is developing the next-generation ion propulsion system with significant enhancements beyond the state-of-the-art in ion propulsion to provide future NASA science missions with enhanced mission capabilities at a low total development cost. As part of a comprehensive thruster service life assessment utilizing both testing and analyses, a Long-Duration Test (LDT) was initiated to verify the NEXT propellant throughput capability to a qualification-level of 450 kg, 1.5 times the anticipated throughput requirement of 300 kg from mission analyses conducted utilizing the NEXT propulsion system. The LDT is being conducted with a modified, flight-representative NEXT engineering model ion thruster, designated EM3. As of June 25, 2008, the thruster has accumulated 16,550 h of operation: the first 13,042 h at the thruster full-input-power of 6.9 kW with 3.52 A beam current and 1800 V beam power supply voltage. Operation since 13,042 h, i.e., the most recent 3,508 h, has been at an input power of 4.7 kW with 3.52 A beam current and 1180 V beam power supply voltage. The thruster has processed 337 kg of xenon (Xe) surpassing the NSTAR propellant throughput demonstrated during the extended life testing of the Deep Space 1 flight spare ion thruster. The NEXT LDT has demonstrated a total impulse of 13.3×10^6 N·s; the highest total impulse ever demonstrated by an ion thruster. Thruster performance tests are conducted periodically over the entire NEXT throttle table with input power ranging 0.5 to 6.9 kW. Thruster performance parameters including thrust, input power, specific impulse, and thruster efficiency have been nominal with little variation to date. This paper presents the performance of the NEXT LDT to date with emphasis on performance variations following throttling of the thruster to the new operating condition and comparison of performance to the NSTAR extended life test.

Nomenclature

BOL	beginning-of-life
DCA	discharge cathode assembly
DCIU	digital control interface unit
DS1	Deep Space 1
DSDRM	Deep Space Design Reference Missions
ELT	Extended Life Test
EM	engineering model
GRC	NASA Glenn Research Center
IPS	ion propulsion system
Isp	specific impulse, s
J_B	beam current, A
J_{DC}	discharge current, A
J_{NK}	neutralizer keeper current, A

LDT	Long-Duration Test
m_C	discharge cathode flowrate, sccm
m_M	main plenum flowrate, sccm
m_N	neutralizer cathode flowrate, sccm
NCA	neutralizer cathode assembly
NEXT	NASA's Evolutionary Xenon Thruster
NSTAR	NASA Solar Electric Propulsion Technology Applications Readiness
P_{IN}	thruster input power, kW
PM	prototype-model
PPU	power processing unit
QCM	quartz-crystal microbalance
RGA	residual gas analyzer
SEP	solar electric propulsion
SOA	state-of-the-art
T	thrust, mN
V_A	accelerator grid voltage, V
V_B	beam power supply voltage, V
V_{DC}	discharge voltage, V
VF–16	Vacuum Facility 16
WT	wear test
Xe	xenon

Introduction

NASA's Evolutionary Xenon Thruster (NEXT), led by the NASA Glenn Research Center (GRC), is being developed to meet NASA's future mission propulsion needs for a more-advanced, higher-power ion propulsion system (IPS) at low total development cost. The success of the NASA Solar Electric Propulsion Technology Applications Readiness (NSTAR) ion propulsion system on Deep Space 1 (DS1) secured the future for ion propulsion technology for future NASA missions (Refs. 1 to 3). In-space propulsion technology analyses conducted at NASA identified the need for a higher-power, higher total throughput capability ion propulsion system beyond the 2.3 kW NSTAR ion thruster targeted for robotic exploration of the outer planets. The NEXT project initially targeted Flagship-class Deep Space Design Reference Missions (DSDRM) such as a Titan Explorer or Neptune orbiter assuming aerocapture at the destinations as the design driver mission applications (Refs. 4 and 5). A refocus study was conducted in 2004 to assess mission benefits of the NEXT IPS for Discovery- and New Frontiers-class missions. Several of the Discovery-class mission studies demonstrated NEXT outperforming the state-of-the-art (SOA) NSTAR, yielding higher net payload mass with fewer thrusters (Ref. 6). Several of the New Frontiers and Flagship-class mission studies showed that NEXT was either mission-enhancing or mission-enabling (Refs. 7 and 8). NEXT technology is applicable to a wide range of NASA solar system exploration missions, as well as earth-space commercial and other missions of national interest. NEXT affords larger delivered payloads and smaller launch vehicle size than chemical propulsion for Discovery, New Frontiers, Mars Exploration, and Flagship outer-planet exploration missions.

The NEXT system consists of a high-performance, 7 kW ion thruster; a high-efficiency, modular, 7 kW power processing unit (PPU)[1] with an efficiency and a specific power greater the NSTAR PPU; a highly-flexible, advanced Xe propellant management system (PMS)[2] that utilizes proportional valves and thermal throttles to reduce mass and volume; a lightweight engine gimbal;[3] and key elements of a digital control interface unit (DCIU)[†] including software algorithms (Refs. 9 to 15). The NEXT thruster and

[1]Power Processing Unit development led by L3 Comm ETI, Torrance, California.
[2]Propellant Management System and DCIU simulator development led by Aerojet, Redmond, Washington.
[3]Gimbal development led by the Jet Propulsion Laboratory and Swales Aerospace.

component technologies demonstrate a significant advancement in technology beyond SOA NSTAR thruster systems. NEXT performance exceeds single or multiple NSTAR thrusters over most of the thruster input power range. The wet propulsion system mass has been reduced by higher-efficiency, higher-specific impulse, and lower specific mass. With a predicted throughput capability more than double that of NSTAR, fewer NEXT thrusters are required compared NSTAR.

Validation of the NEXT thruster service life capability is being addressed via a comprehensive service life validation scheme utilizing a combination of test and analyses. A NEXT service life assessment was conducted at NASA GRC employing several models to evaluate all known failure modes incorporating the results of the NEXT 2,000 h wear test (WT) conducted on a NEXT engineering model (EM) ion thruster at 6.9 kW input power (Refs. 16 and 17). The assessment predicts the earliest failure occurring sometime after 750 kg of Xe throughput, well beyond the mission-derived propellant throughput requirement of 300 kg (Ref. 17). To validate the NEXT thruster service life model and qualify the NEXT thruster, the NEXT Long-Duration Test (LDT) was initiated. The purpose of the NEXT LDT is to: 1) characterize thruster performance over the test duration, 2) measure the erosion rates of critical thruster components, 3) identify unknown life-limiting mechanisms, and 4) demonstrate 1.5 times the mission-derived propellant throughput requirement resulting in a qualification propellant throughput requirement of at least 450 kg. In addition to the NEXT LDT, multiple component-level lifetime tests are underway or planned for the NEXT program to augment the results of the LDT (Ref. 18). The NEXT thruster service life analysis is being updated based upon the LDT data and component testing findings as well as being applied for potential mission opportunities to assess thruster wear and performance (Ref. 19).

The thruster operation has been carried out in a multi-phase approach: phase 1) quick sprint at full power to verify extended duration functionality and validate end-of-life prediction, phase 2) thruster operation in a throttled mission-representative profile that focuses on operating points of interest with regard to wear characteristics and life-limiting phenomena, phase 3) operation to failure at the thruster operating point with the shortest lifetime, i.e., full-input power. Phase 1 operation has been completed demonstrating 13,042 h of operation at the full-input-power with performance and erosion characteristics supporting the thruster lifetime throughput capability predicted by the NEXT service life assessment of ~750 kg. Phase two operation has begun and to date 3,508 h of operation at 4.7 kW input power has been demonstrated.

Test Article

A The NEXT LDT is being conducted with an engineering model ion thruster, designated EM3, shown in Figure 1. The EM3 thruster has been modified to a flight-representative configuration so it is more comparative to the NEXT prototype-model (PM) thruster by incorporating PM ion optics and a graphite discharge cathode keeper electrode (Ref. 14). To reduce the risk of a facility-induced failure of the thruster, the neutralizer assembly was enclosed to protect insulators from sputter deposition and all critical surfaces were grit-blasting for flake retention. The PM ion optics beam extraction diameter was reduced from the 40 cm diameter of the EM thrusters to 36 cm diameter to reduce outer-radius accelerator aperture erosion caused by beamlet over-focusing in these low current density regions (Refs. 16, 20, and 21). Reducing the ion optics beam extraction diameter from 40 cm also reduces the maximum thruster beam divergence and neutral loss rate without a significant increase in discharge losses (Ref. 9). The PM ion optics geometry retains many of the key features of the EM design, however, improved manufacturing techniques implemented by a new vendor led to: better control of aperture variation as a function of grid radius, a reduced and more consistent cusp profile, and elimination of “worm track” surface problems previously encountered (Ref. 14). The aperture variation for the PM accelerator grid is +1/–6 percent compared to +11/–16 percent for EM optics (Ref. 14). The PM ion optics mounting scheme has been altered to eliminate the buildup and relaxation of assembly and thermally-induced stresses that lead to the decreasing ion optics’ grid-gap with test duration (Refs. 16, 22, and 23).

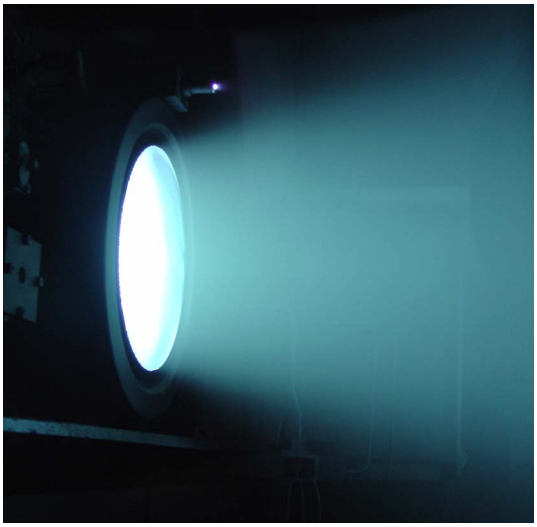

Figure 1.—NEXT EM3 operating at full-power during the Long-Duration Test.

One of the unexpected findings from the NSTAR Extended Life Test (ELT) was the anomalous discharge cathode keeper erosion, which was more severe and qualitatively different than prior 1,000 h and 8,200 h NSTAR wear tests (Refs. 22, 24, and 25). Due to the complete NSTAR ELT discharge cathode keeper faceplate erosion and the NEXT EM 2,000 h wear test results, a graphite discharge cathode keeper is employed on EM3, similar to the NEXT PM thruster design, to mitigate keeper erosion. The erosion rate of carbon due to the low-energy discharge plasma ion impacts is over 20 times lower than molybdenum (Ref. 26), thus utilization of a graphite keeper electrode dramatically extends thruster service life.

The NEXT thruster, shown operating in Figure 1, is nominally a 0.5 to 6.9 kW input power Xe ion thruster with 2-grid ion optics with screen (+) upstream and accelerator (–) downstream electrodes. The technical approach for the NEXT design is a continuation of the derating philosophy used for the NSTAR ion thruster. A beam extraction area 1.6 times NSTAR allows higher thruster input power while maintaining low voltages and ion current densities, thus maintaining thruster longevity. The semi-conic discharge chamber utilizes a hollow cathode emitter with a ring-cusp magnetic topology created by high-strength, rare earth magnets for electron confinement. A flake retention scheme identical to that employed on the NSTAR thruster enhances the adhesion of thin films to the discharge chamber surfaces (Ref. 27). New, compact propellant isolators with higher voltage isolation capability than those used by the NSTAR thruster are utilized. The NEXT neutralizer design is mechanically similar to the International Space Station Plasma Contactor leveraging this extensive database to reduce risk. Additional description of the NEXT EM3 thruster design can be found in References 28 to 32.

Test Support Hardware

The following section briefly describes the NEXT LDT supporting hardware. More detailed descriptions can be found in References 16, 32 to 34.

Vacuum Facility and Facility Diagnostics

The NEXT LDT is being conducted in the 2.7 m diameter by 8.5 m long Vacuum Facility 16 (VF–16) at GRC, shown in Figure 2. VF-16 has an emergency bell jar on the end cap into which the thruster can be withdrawn and isolated in the event of a facility emergency. VF-16 is equipped with 10 cryogenic pumps for nominal thruster operation and an additional cryo-pump on the isolated bell jar for emergency use.

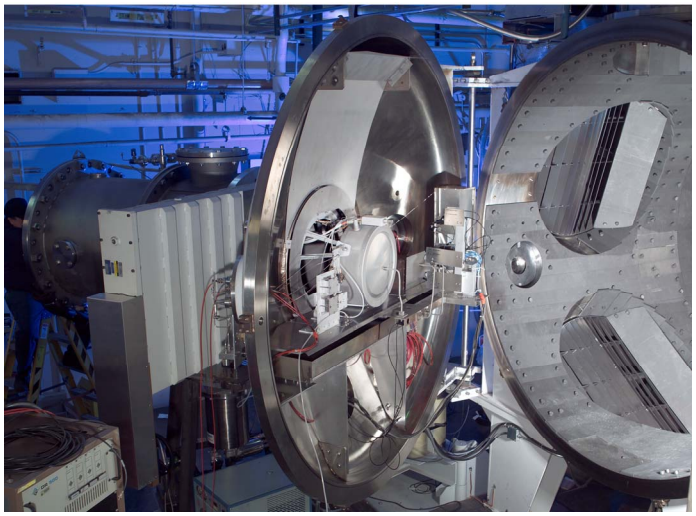

Figure 2.—VF–16 at GRC—end-cap opened. EM3 extends out the emergency bell jar in testing configuration.

With all 10 cryo-pumps operating, the base pressure is less than 3×10^{-7} torr. Facility pressure is monitored by two ionization gauges, a glass-tube ion gauge located on the facility wall 0.5 m downstream of the thruster and a dual-filament nude near-thruster ion gauge mounted 0.5 m radially beside EM3. In addition, the isolated bell jar has an ion gauge that is turned off during normal operation. The measured facility pumping speed, corrected for Xe, is 180 kL/s using the wall-mounted ion gauge. With 10 operational cryo-pumps, the near-thruster background pressure is 2.5×10^{-6} torr, corrected for Xe, when the thruster is operating at full-power. A quadrupole residual gas analyzer (RGA) measures and records the quantity of individual gas species inside VF–16 continuously every minute. All interior surfaces downstream of the thruster are lined with 1.2 cm thick graphite paneling to reduce the back-sputtered material flux to the thruster and test support hardware. The back-sputter rate, nominally 3 μm/khr when the thruster is at full-power, is monitored by a quartz-crystal microbalance (QCM) located next to the ion thruster. Three pinhole cameras are mounted next to the QCM and will be microscopically analyzed at the conclusion of the life test to determine the source of back-sputtered material. In addition to the pinhole cameras, five quartz witness plates are mounted along the length of the vacuum chamber wall.

Thruster Diagnostics

A computerized data acquisition and control system is used to monitor and record ion engine and facility operations. Data are sampled at a frequency range of 10 to 20 Hz and stored every minute during normal operation. A set of data consists of individual mass flow rates, ion engine currents measured with current shunts, voltages measured with voltage dividers, facility pressures, and the QCM measurement. As part of the periodic thruster characterization, the thruster is connected to an electrically floating power supply circuit used to determine screen grid ion transparency and discharge keeper ion current. The circuit electrically ties the screen grid or discharge keeper to the discharge cathode during normal operation, but biases the screen grid or discharge keeper negative relative to discharge cathode potential to repel electrons and measure the collected ion current.

Ion beam diagnostics include three staggered planar probes mounted onto a translation stage to measure radial ion current density profiles and an ExB probe, or Wien Filter, to measure the doubly-to-singly charged ion signature. Each molybdenum Faraday probe has 1-cm^2 circular current-collection area and is biased –30 V relative to facility ground to repel electrons. Faraday probes are fixed at axial positions of 20, 173, and 238 mm downstream of the accelerator grid. The collected currents are measured through separate isolated shunt resistors. The ExB probe is positioned 7.6 m downstream of the thruster on centerline, yielding a doubly-to-singly charged ion signature in the far-field. The ExB probe

design is described in Reference 35. The Faraday probes and ExB probe are protected from the high-energy ion beam by parking the probes outside the beam and behind a graphite shutter, respectively. The LDT ion beam diagnostics are described in detail in Reference 34.

Operating Conditions

The NEXT ion thruster is designed for solar electric propulsion (SEP) applications that experience variation in power available as solar flux changes at various distances from the sun throughout the mission. Ion thruster input power is designed to be throttled from 0.5 to 6.9 kW to accommodate this variation in available power. The NEXT LDT consists of three operating phases: 1) operate at the full-power point until 267 kg propellant throughput has been demonstrated, 2) throttle to assess extended operation at operating conditions of interest after 267 kg, and 3) throttle to full-power until either decision is made to end the test or the thruster fails. The LDT is currently in Phase 2 of thruster operations and has operated at full-power and the first throttled operating condition. The thruster full-input-power (6.9 kW) operating condition and first throttled operating condition (4.7 kW) are shown in Table 1. The input power indicated in Table 1 is a nominal operating power requirement from the NEXT throttle table at the thruster beginning-of-life and may differ slightly from thruster to thruster (Ref. 29).

TABLE 1.—NEXT LDT FULL-INPUT-POWER AND FIRST THROTTLED OPERATING CONDITIONS

P_{IN}, kW[a]	J_B, A	V_B, V	V_A, V	m_M, sccm	m_C, sccm	m_N, sccm	J_{NK}, A
6.83	3.52	1800	–210	49.6	4.87	4.01	3.00
4.68	3.52	1180	–200	49.6	4.87	4.01	3.00

[a]Nominal value.

The proposed NEXT LDT throttling strategy is illustrated in Table 2 with operating durations subject to change if erosion or performance trends differ from projections. This throttling strategy demonstrates operation over the extremes of the NEXT throttling table including: highest power, highest total accelerating voltage, highest thermal load, condition with worst under-focusing at center-radius aperture location, condition with worst over-focusing at outer-radius locations, lowest power, lowest total accelerating voltage, lowest thermal load, and the condition with the highest ratio of discharge cathode emission to discharge cathode flow rate. Thruster performance is measured periodically over the entire throttle table regardless of thruster operating condition. Performance characterization tests are conducted to assess performance of the thruster and thruster components at multiple power levels that envelope the entire NEXT throttle table, listed in Table A.1 of the Appendix. Periodic component performance assessments of the discharge chamber, ion optics, and neutralizer cathode are performed at the various thruster operating conditions. Ion optics performance includes electron backstreaming, perveance, and screen grid ion transparency measurements. Discharge chamber performance is assessed by measuring discharge losses as a function of discharge propellant utilization efficiency for fixed discharge voltages. Neutralizer performance is evaluated by measuring dc keeper voltage, ac keeper voltage, and ac keeper current as a function of neutralizer flow for a fixed neutralizer current.

TABLE 2.—NEXT LDT PROPOSED THROTTLING STRATEGY

P_{IN}, kW[a]	J_B, A	V_B, V	Duration, kh	Segment throughput, kg	Segment total impulse, N·s
6.83	3.52	1800	13	267	1.11×10^{7}
4.68	3.52	1180	4	82	2.76×10^{6}
1.51	1.20	1020	2	19	5.80×10^{5}
6.83	3.52	1800	3	62	2.55×10^{6}
0.529	1.00	275	3	20	2.75×10^{5}
2.43	1.20	1800	2	15	5.78×10^{5}
		Totals	27	465	1.78×10^{7}

[a]Nominal value.

Thruster Performance

As of June 25, 2008, the NEXT EM3 thruster has accumulated 16,550 h of operation. The NEXT thruster has processed 337 kg of Xe illustrated in Figure 3; *surpassing the total propellant throughput processed by the DS1 flight spare in the NSTAR ELT (235 kg)*. The NEXT thruster has processed more than 4.5 times that of the Deep Space 1 NSTAR flight thruster. Figure 3 shows the NEXT LDT propellant throughput as a function of elapsed time with reference to the NSTAR ELT and flight DS1 thruster, the thruster throughput requirements from various mission analyses conducted using the NEXT propulsion system, and the NEXT qualification level throughput—450 kg (Refs. 23, 36, and 37). The NEXT thruster has demonstrated a total impulse of 13.3×10^6 N·s to date; *the highest total impulse ever demonstrated by an ion thruster.* The NEXT milestone is also the highest total impulse ever demonstrated by an electric propulsion device with an input power less than 10 kW (Ref. 38). The NEXT LDT total impulse demonstrated exceeded that of the 30,000 h NSTAR ELT in less than 1/3rd the thruster operating duration, shown in Figure 4.

Performance of the thruster has been steady with minimal degradation. Erosion of critical thruster components has been within modeling predictions and consistent with the NEXT service life assessment (Refs. 19, 39, and 40). Several of the NSTAR ELT-observed wear anomalies have been significantly reduced and in most cases eliminated. There has been no observed discharge cathode keeper orifice erosion, no measured increase in accelerator grid aperture cusps except for the outer edge apertures, and no measured change in the cold grid-gap of the ion optics for the NEXT engine—all of which were observed during the NSTAR ELT of the DS1 flight spare (Ref. 23). NEXT LDT erosion characteristics and thruster lifetime predictions are incorporated in References 19 and 39.

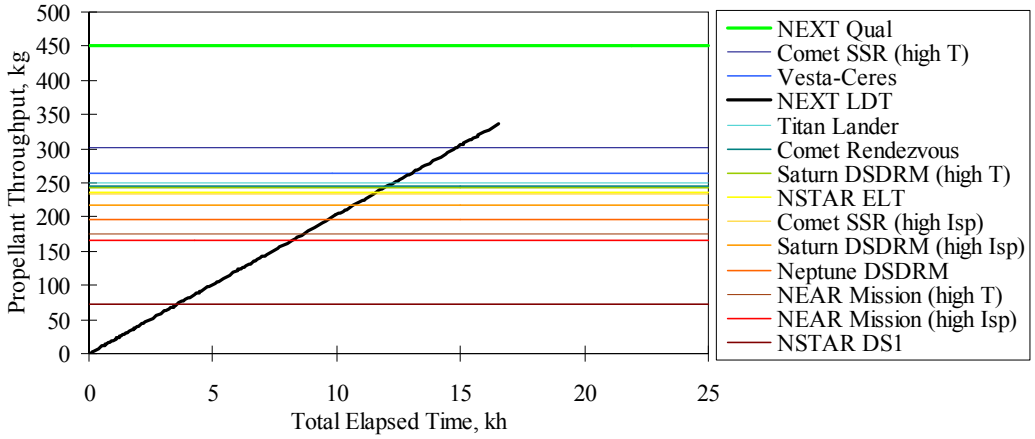

Figure 3.—NEXT LDT propellant throughput data as a function of time with reference milestones.

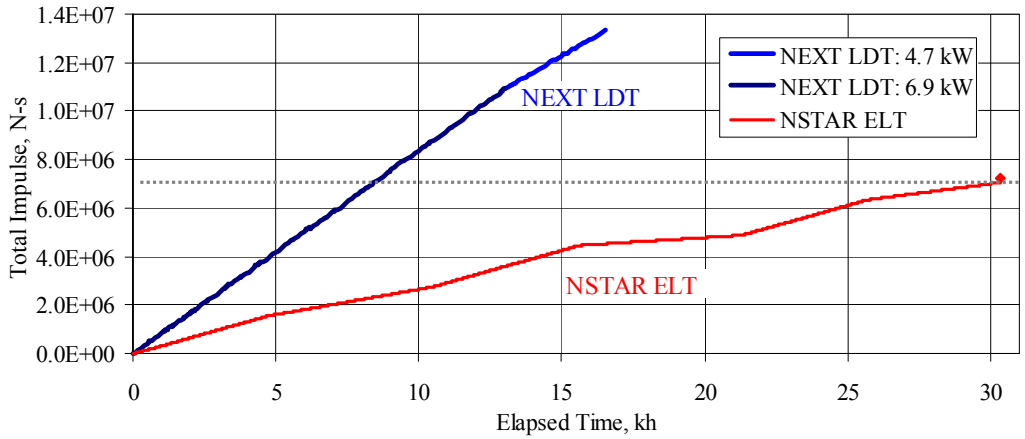

Figure 4.—NEXT LDT and NSTAR ELT total impulse data as a function of time (Ref. 25).

The following section describes the observed trends in thruster performance at the full-input-power (6.9 kW) operating point, at the first throttled operating condition (4.7 kW), and during the performance characterization tests conducted periodically at operating conditions spanning the complete the NEXT throttle table.

Engine Performance

Thruster performance parameters that are important for mission planning such as thrust, specific impulse, input power, and efficiency are plotted as a function of time in Figure 5 to Figure 8. In most of the performance graphs, data are grouped according to values of beam current and beam power supply voltage. For thrust calculations, the beam divergence thrust correction factor and the total doubly-to-singly-charged ion current ratio ranged from 0.962 to 0.975 and 0.028 to 0.060, respectively, based upon the methodology developed for NSTAR thrusters (Ref. 41). At the full-power operating condition, the beam divergence thrust correction factor and the total doubly-to-singly-charged ion current ratio are assumed to be 0.975 and 0.043, respectively. Ingested mass flow due to facility background pressure was included in the total mass flow rate to the engine for determining specific impulse and thrust efficiency (Ref. 42). At full-power, thrust and specific impulse have remained constant at values of 237 ± 3 mN and 4170 ± 70 s, respectively. The indicated uncertainty in thruster performance values are discussed in Reference 43. Since throttling to the 4.7 kW operating condition, thrust and specific impulse from the runtime data have remained constant at values of 192 ± 2 mN and 3380 ± 60 s, respectively. Noise in the runtime data is predominantly due to changes in the beam current, which is maintained by manually adjusting the discharge current. Spikes in the data are due to thruster shutdowns and restart events. At full-power, thrust efficiency decreased from the beginning-of-test value of 0.710 to 0.706 after 13,042 h due to an increase in input power to the thruster from 6.85 to 6.87 kW. At 4.7 kW, thrust efficiency decreased from the beginning-of-throttled-segment value of 0.677 to 0.676 after 3,508 h. The increase in thruster input power is a result of increasing thruster discharge losses as the discharge chamber neutral loss rate increases from accelerator aperture erosion. Increases in specific impulse and thrust efficiency are observed for many operating conditions after the beginning-of-test characterization due to an intentional decrease in neutralizer flow to improve overall propellant utilization efficiency. Trends at all operating conditions are similar: constant thrust, constant specific impulse after the neutralizer flow decrease at beginning-of-test, slightly increasing input power due to increasing discharge losses, and slightly decreasing efficiency (after neutralizer flow decrease) due to increasing input power.

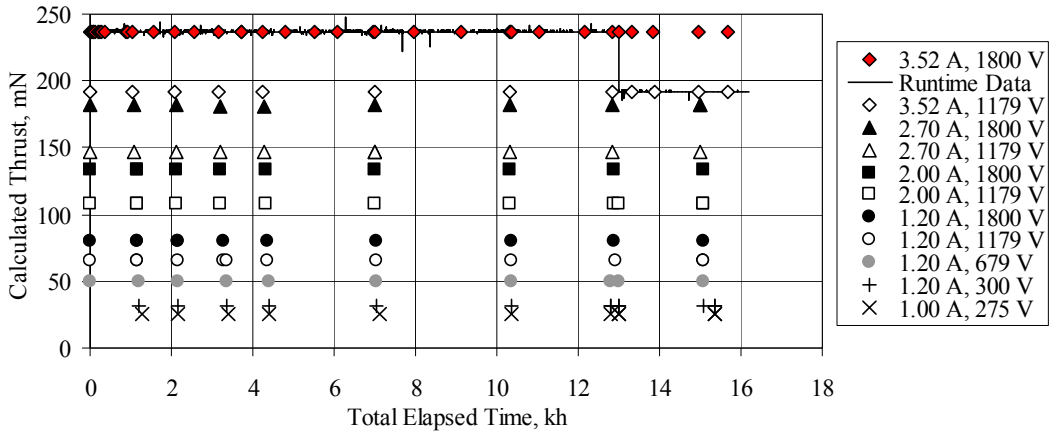

Figure 5.—Calculated thrust data as a function of time.

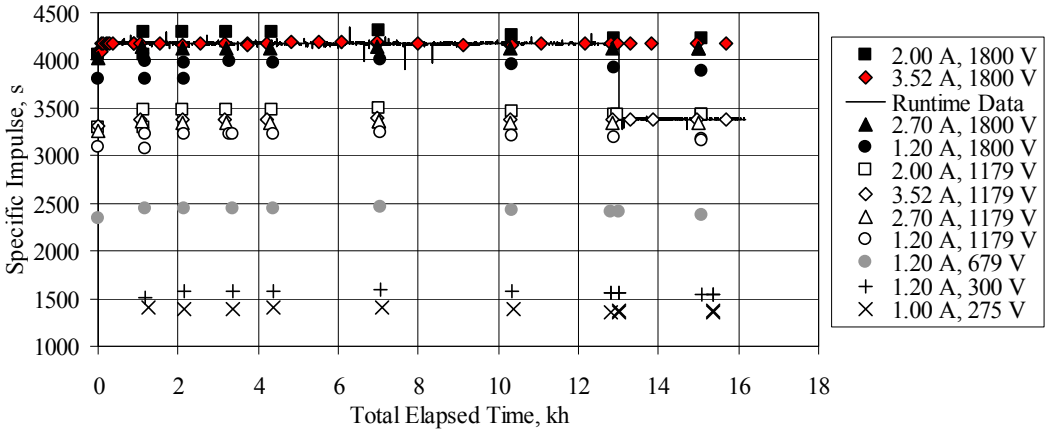

Figure 6.—Specific impulse data as a function of time.

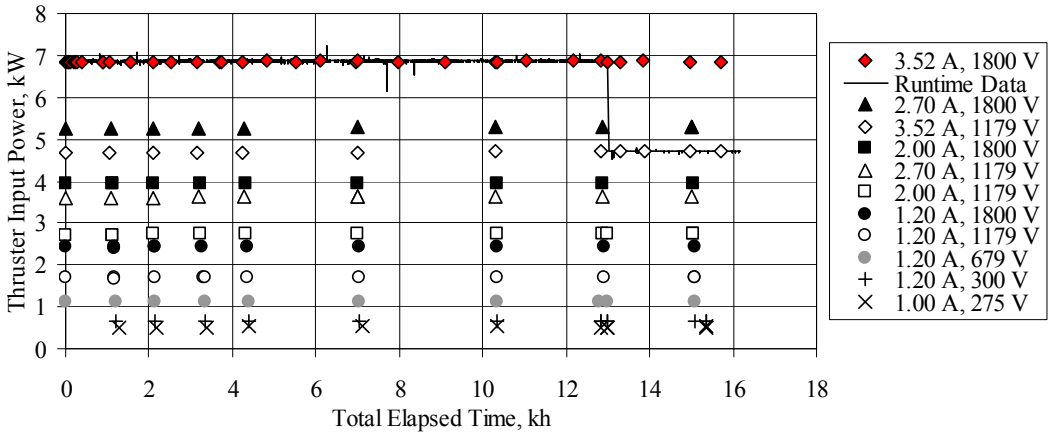

Figure 7.—Thruster input power data as a function of time.

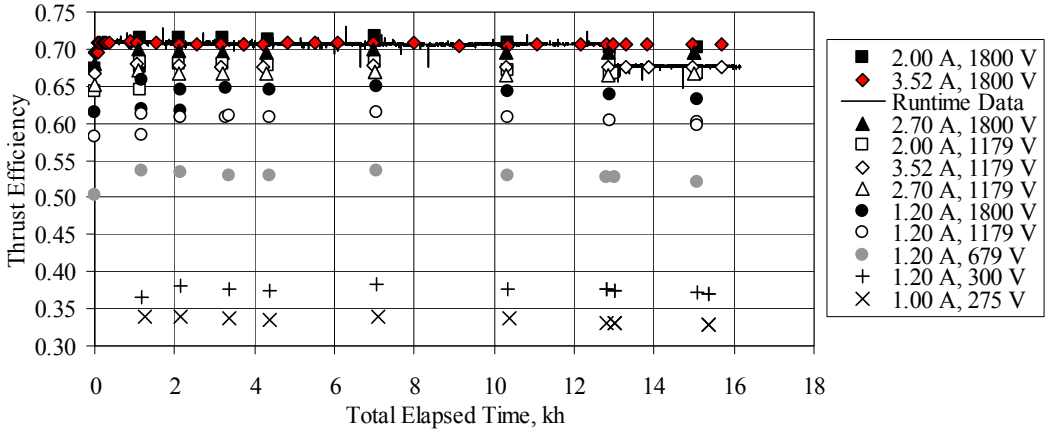

Figure 8.—Thrust efficiency data as a function of time.

Discharge Chamber

The discharge cathode and main plenum flow rates are set according to the NEXT throttle table, Table A.1, which for both the full-power and 4.7 kW operating conditions are 4.87 and 49.6 sccm, respectively. Discharge propellant utilization efficiency and discharge losses are plotted as a function of

time in Figure 9 and Figure 10, respectively. Constant discharge propellant utilization efficiencies are observed at all operating conditions. At full-power and 4.7 kW, discharge propellant utilization efficiency, which is the beam current divided by discharge propellant flow rate (including ingested flow) in equivalent amperes, has been constant at 0.89. Discharge losses are lowest for the full-power operating condition and increase with decreasing total voltage, i.e., the sum of the absolute values of the beam and accelerator power supply voltages. That the discharge losses increases with decreasing total voltage for constant beam current is largely due to a decreasing screen grid ion transparency (Ref. 30). Full-power discharge loss, discharge power divided by the beam current, has risen from 123 to 131 W/A over the 13,042 h of operation. Discharge losses plateau'd after ~7,000 h of operation consistent with similar trends in accelerator aperture erosion and have remained constant since (i.e., up to 16,550 h of operation (Ref. 39)). Since throttling, thruster discharge losses at 4.7 kW have remained approximately constant at 142 W/A. Modest increases in discharge losses, ≤ 6 percent, are observed for each of the operating conditions over the total test duration.

Figure 11 shows discharge losses as a function of discharge propellant utilization efficiency for full-power and a low-power operating condition throughout the wear test. The ratio of main to discharge cathode flow rate is adjusted to maintain the nominal discharge voltage. No significant changes in the functional dependence of discharge losses on propellant utilization efficiency are observed over time. Shifting of the curves up by ~8 W/A at full-power is consistent with the increase in runtime data discharge losses.

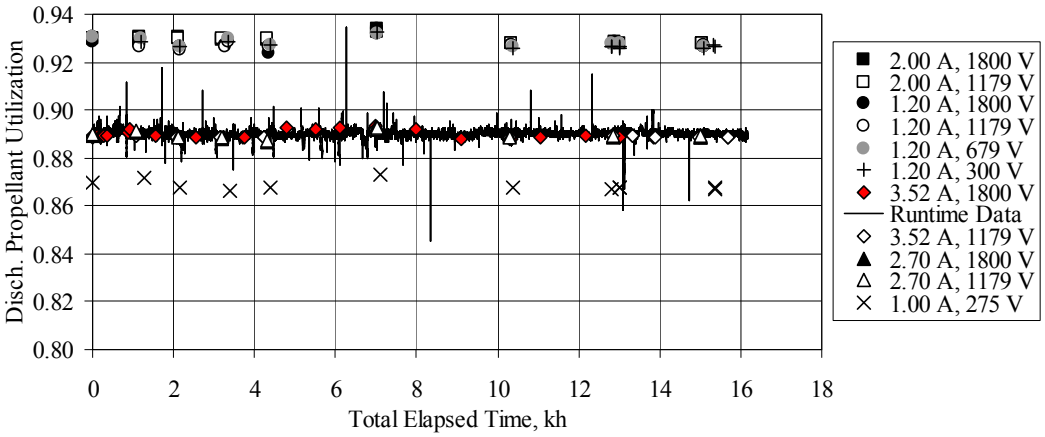

Figure 9.—Discharge propellant utilization efficiency (including mass ingestion, but no doubly-charged ions) as a function of time.

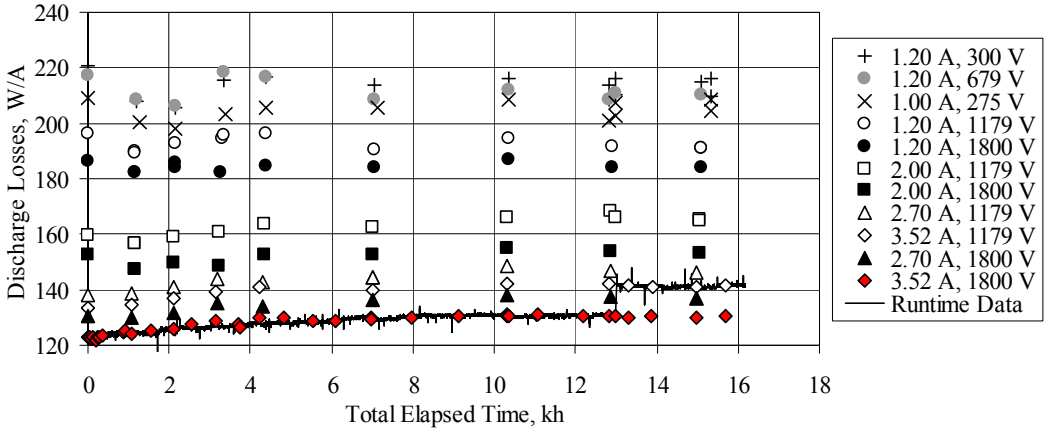

Figure 10.—Discharge loss data as a function of time.

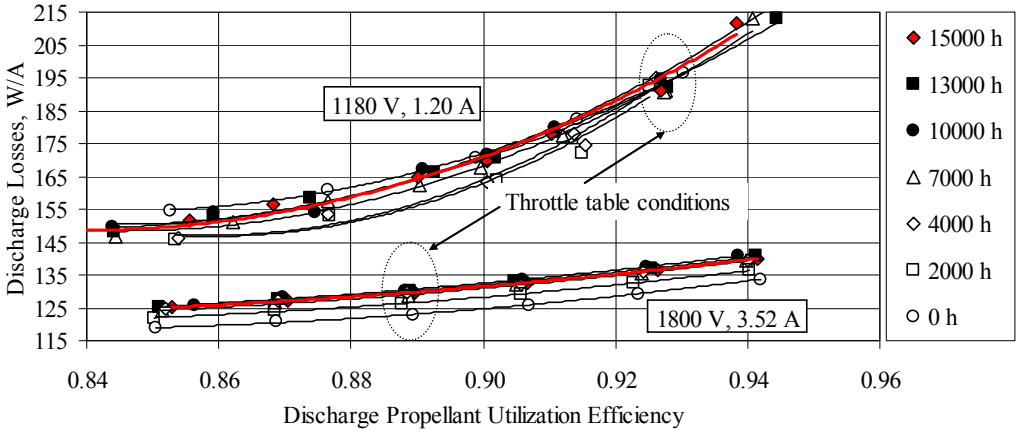

Figure 11.—Discharge losses plotted against discharge propellant utilization efficiency (including mass ingestion) for full-power and low-power conditions after various test durations with fixed discharge voltages of 23.5 ±0.5 V and 26.0 ±0.5 V, respectively.

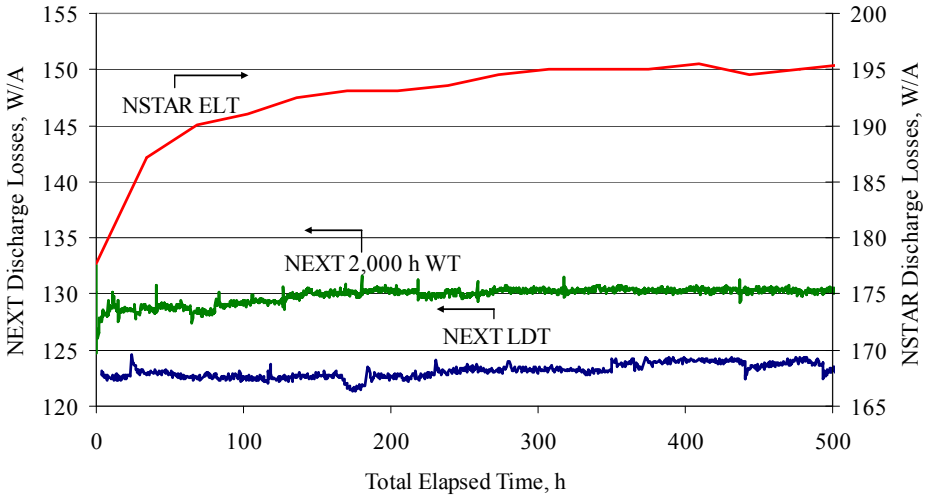

Figure 12.—Discharge losses for the NSTAR ELT, NEXT 2,000 h wear test (WT), and NEXT LDT (Refs. 44 and 52).

The NEXT LDT gradual 6 percent increase in discharge losses is in contrast to the larger and more rapid beginning-of-test increase in discharge losses exhibited by the NSTAR thruster. NSTAR thruster full-power discharge losses, considerably higher (~50 W/A) than NEXT due primarily to the smaller discharge chamber, increased by 10 to 15 W/A within the first 500 h of operation in three separate wear test (Refs. 22, 24, and 44). The NEXT thruster initial change in discharge losses has been small compared to that of NSTAR thrusters during the NEXT LDT and the NEXT 2,000 h wear test, illustrated in Figure 12, resulting in more constant thruster input power and thrust efficiency at the beginning of life (Refs. 16, 22, 24, 44, and 45). The reduced beginning-of-life (BOL) increase in discharge losses in the NEXT design is a result of a flatter NEXT beam profile, thicker accelerator grid, smaller cusp ion optics, and more focused beamlets at the full-power operating condition. Furthermore, the ~2 W/A LDT initial increase in discharge losses are less than the ~5 W/A increase observed in the NEXT 2,000 h wear test due to the incorporation of PM ion optics on the EM3 thruster. The PM optics have reduced cusp size, increased aperture uniformity compared to EM optics, and 36 cm diameter active area (removing the outer 2 cm apertures where over-focusing occurs), which reduce the BOL increase in discharge losses (Ref. 14). After 337 kg, the NEXT LDT full-power discharge losses increased by 8 W/A compared to the NSTAR ELT increase of 22 W/A after 210 kg (Refs. 25and 45).

Discharge voltage and current runtime data and characterization data for each of the thruster performance operating conditions are shown in Figure 13 and Figure 14, respectively. Full-power discharge current and voltage increased from 18.6 A and 23.3 V to 19.3 A and 23.9 V after 13,042 h of operation, respectively. Full-power discharge voltage has continued to increase to 24.1 V after 3,508 h at 4.7 kW (total operating duration of 16,550 h). The discharge current at full-power has actually decreased to 19.0 A since throttling to the new operating condition. The cause of the reduction in discharge current at full-power is a discharge keeper-to-common short that appeared after 13,875 h of operation (833 h after throttling to 4.7 kW). The discharge voltage and current runtime data at 4.7 kW demonstrate a step increase from 24.3 to 24.5 V and step decrease from 20.5 to 20.3 A, respectively, caused by the keeper short. Since the short, the discharge voltage at 4.7 kW has remained constant, while the discharge current has slowly increased to 20.4 A as a result of the observed accelerator aperture erosion (Ref. 39). The shorting of the discharge keeper to common was an expected event based upon the findings from the NEXT 2,000 h WT and the HiPEP 2,000 h WT (Refs. 16 and 46). Post-test analyses measured material deposits on the upstream surface of the keeper faceplate near the orifice of 40 and 70 μm thicknesses for the NEXT and HiPEP wear tests, respectively(Refs. 47 and 48). Assuming linear growth, extrapolation of these thicknesses for extended duration would have resulted in bridging the estimated operating gap between the NEXT LDT keeper and cathode face after an operating duration on the order of 10 to 20 kh. The short appeared in the NEXT LDT after 13.9 kh, within the bounds of the two deposition rates. It should be mentioned that the NEXT lifetime assessment also predicted a priori this shorting event and considered its impact on thruster service life (Refs. 19 and 40).

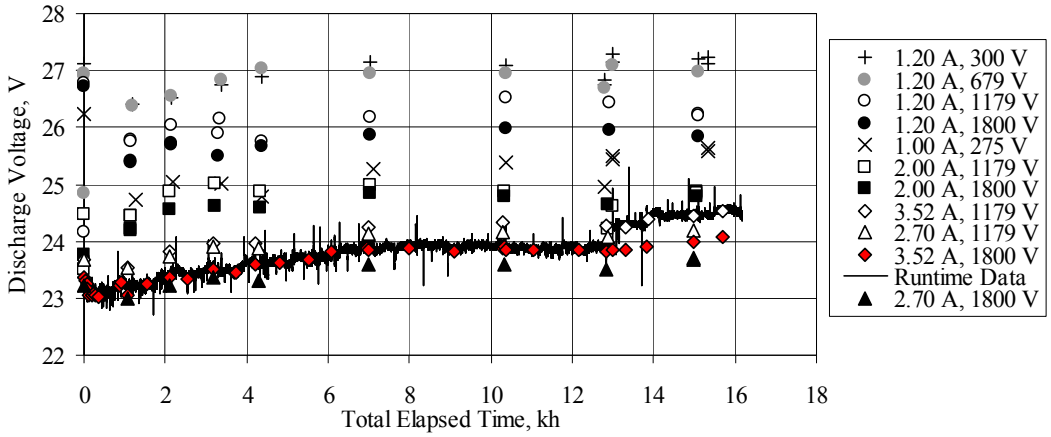

Figure 13.—Discharge voltage data as a function of time.

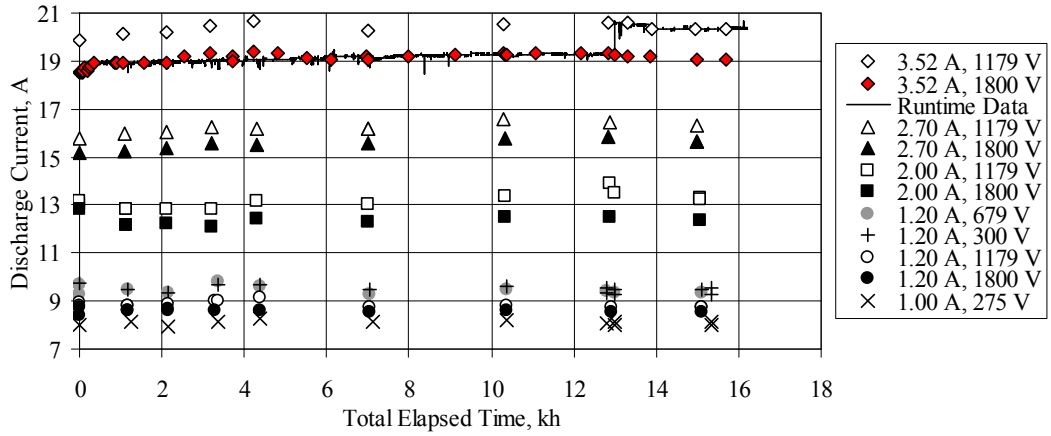

Figure 14.—Discharge current data as a function of time.

The increasing discharge current, required to maintain a constant beam current due to increasing neutral transparency as accelerator apertures erode, is expected from past ion thruster wear testing (Refs. 22 and 25). An increase in discharge current produces an increase in the discharge primary electron number density offsetting the reduction in discharge chamber neutral number density to maintain the same discharge chamber ion production. As shown previously, it is possible to use accelerator aperture erosion measurements to predict the change in discharge current required to maintain the beam current (Refs. 49 and 50). The beginning-of-test decrease and overall 3 percent increase in discharge voltage may be influenced by the following: chamfering of the upstream screen grid aperture edge, the buildup of a resistive coating on the discharge chamber, changes in neutral density and electron temperature caused by increasing neutral transparency, changes in the electron emitter surface conditions or heat transfer, periodic emitter oxygen exposure due to graphite keeper moisture absorption during facility regenerations, shorting of the discharge cathode keeper to cathode common, or other changes in the discharge chamber conditions (Ref. 23). The overall trends for each operating condition with time are similar to that of the full-power test condition, namely increases in voltage and current of a few percent. The beginning-of-test decrease in discharge voltage is more pronounced for the lower-power operation conditions.

Figure 15 shows the discharge keeper voltage and discharge keeper ion saturation current as a function of time at full-power. These parameters directly impact the discharge keeper wear rate. The keeper ion saturation current increased by ~5 percent after ~13 kh of operation at full-power, consistent with the observed increase in discharge current and indicates an increase in localized ion density near the discharge cathode assembly (DCA). The discharge keeper voltage increased from 4.3 to 5.3 V over the first 13,042 h of operation of the test following the observed increase in discharge voltage from 23.3 to 23.9 V. Due to the increasing discharge keeper voltage the potential between discharge ions and the keeper had been decreasing leading to a slight reduction in the discharge keeper wear rate at full-power. The NEXT LDT full-power discharge keeper ion saturation current and voltage are similar to the NEXT 2,000 h wear test values, thus it is anticipated that both test articles would be exposed to similar levels of ion impingement (Refs. 16 and 20). Since 13,875 h, the discharge cathode keeper has demonstrated a thermally-dependent short to cathode common. The onset of this shorting event is consistent with the NEXT thruster service life assessment and previous wear test experiences (Refs. 17 and 25). As a result of the shorting event, no ion saturation current data are available for conditions of high emission current, i.e., when the keeper is shorted, because the keeper cannot be biased with respect to cathode common. The conditions at which shorting has been observed to date are illustrated in Figure 16 as well as discharge keeper voltages for performance operating conditions.

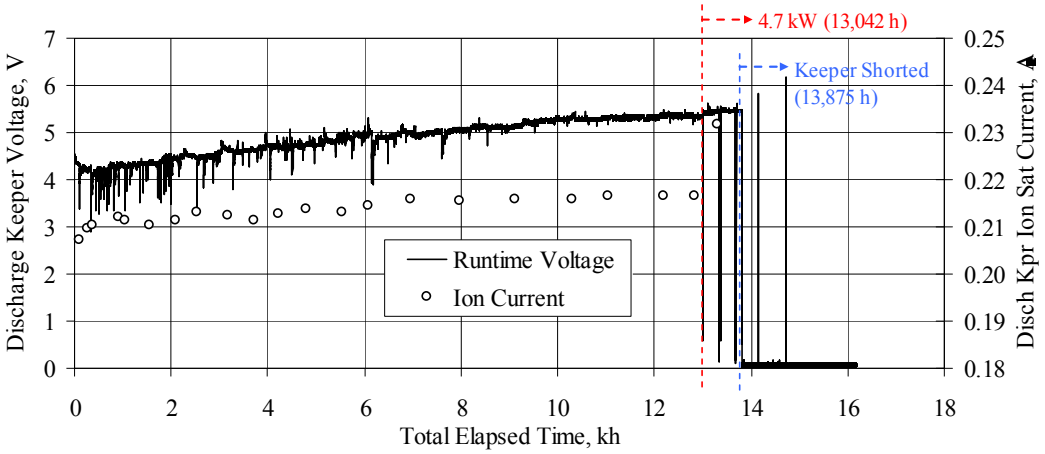

Figure 15.—Full-power discharge keeper voltage and ion saturation current data.

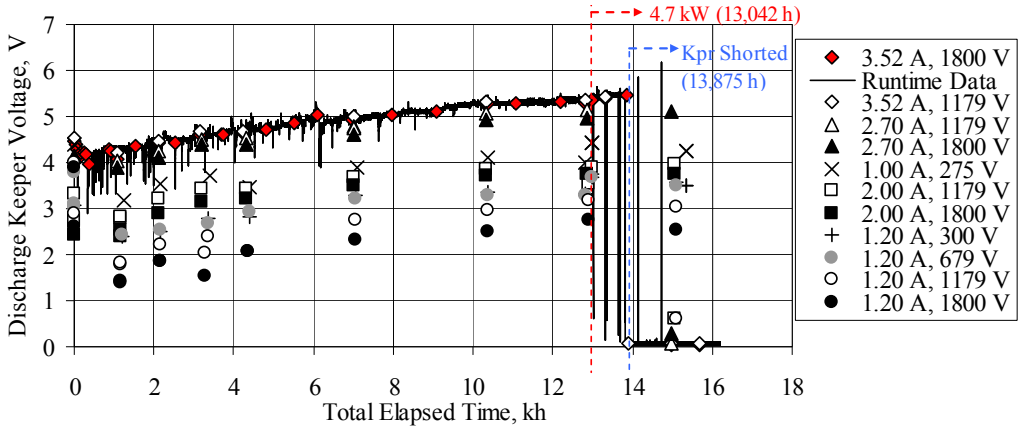

Figure 16.—Discharge keeper voltage data as a function of time.

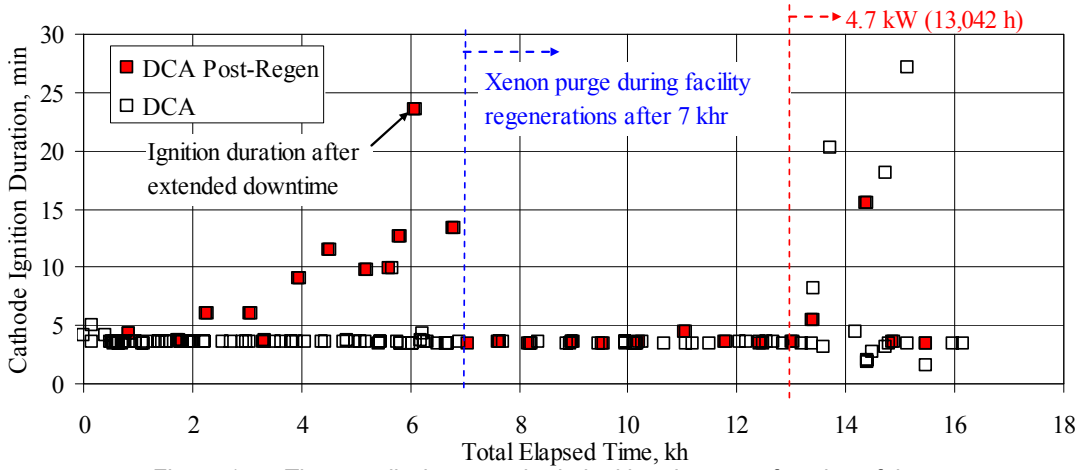

Figure 17.—Thruster discharge cathode ignition data as a function of time.

Discharge cathode ignition durations, 159 total to date, are plotted as a function of elapsed time in Figure 17. With the exception of the post-facility-regeneration ignitions, all discharge cathode ignitions up to 13,042 h had been less than 5 minutes. After 2,000 h, the post-cryopump-regeneration ignition durations began to be increase with thruster operating time. The highest ignition duration, ~24 min, occurred following an extended period of thruster downtime for cryo-pump repairs. After 7,000 h of operation, a Xe purge of 4.00 sccm discharge cathode flow was maintained during the facility regenerations in order to maintain collisional flow inside the cathode tube. The purge flow effectively reduced the post-facility-regeneration ignition durations to their nominal values. The exact cause of the post-regeneration increased ignition durations is unknown, but is a result of facility effects due to exposure to pressures up to 100 mTorr during regenerations. One possibility is absorption of moisture on internal surfaces of the graphite keeper, which acts as a getter for moisture during the facility regeneration when facility pressure reaches 100 mTorr. This moisture would not necessarily be driven off by the cathode conditioning sequence utilized prior to ignition. Metallic keeper material previously used in NEXT and NSTAR thrusters would not collect moisture as effectively as carbon, thus this behavior was not previously observed. The absorbed moisture may be released during the subsequent cathode ignition exposing the emitter to higher levels of moisture and oxygen. This exposure may also be responsible for the increase in discharge voltage previously discussed. The cathode purge flow may be reducing moisture absorption on the interior surfaces of the keeper and orifice. Regardless, a flight thruster in space would not experience this type of repeated exposure and therefore this issue is limited to ground-based testing.

Shortly after throttling to the new operating condition (369 h), a thermally-induced high-impedance was observed on the discharge cathode heater. The high-impedance was observed intermittently during cathode conditioning sequences and ignitions, resulting in a momentary inability to draw the required heater current. As a result of this behavior, the discharge cathode ignition durations experienced large variability after 13,411 h of thruster operation. Some ignitions were performed with application of discharge power sooner than 3.5 min while the thruster was hot illustrating ignition times of only a few minutes, while occasional high-impedances were frequent enough and of long enough duration to cause ignition durations of several tens of minutes. The cause of this behavior has been investigated and determined due to be the combined effects of a resistive layer formation between the heater sheath and cathode tube and a thermally-induced gap formation between the heater sheath and cathode tube both contributing to an intermittent break in the heater current return path. The high-impedance behavior followed a high-pressure event while the thruster was hot (causing resistive layer formation) and shortly after throttling to the new operating condition with a higher discharge cathode emission current (breaking of previously established diffusion bond and/or thermally induced gap formation). After the investigation, it was speculated that continued operating at the 4.7 kW operating condition could result in re-establishing a good current return path through diffusion bonding of the heater outer-sheath to the cathode tube. Since 15,128 h, the intermittent high-impedance has not been observed likely due to diffusion bonding of the heater sheath to the cathode tube at the new operating condition. The NEXT PM design incorporates a positive heater current return via a physical, solid connection between the two surfaces that prevents this behavior from occurring (Ref. 14).

Neutralizer

Neutralizer flow and neutralizer keeper current are set to 4.01 sccm and 3.00 A, respectively, for both the full-power and 4.7 kW operating conditions. Neutralizer keeper voltage, relative to neutralizer cathode common, and the coupling voltage, which is neutralizer cathode common relative to vacuum facility ground, are plotted as a function of time in Figure 18. Since the beam current is 3.52 A for both operating conditions, there is no discernable difference between operations of the neutralizer at these two conditions (i.e., same flow rate, current, and similar accelerator grid voltages results in similar neutralizer voltages). The keeper voltage has decreased slightly from 11.2 to 10.7 V over 16,550 h. This observed behavior is likely due to changes in the neutralizer orifice geometry leading to changes in neutralizer internal pressure. As with most of the thruster runtime data, “spikes” are observed in the neutralizer keeper voltage corresponding to engine restarts, which is similar to NSTAR wear test and NEXT 2,000 h wear test neutralizer behavior (Refs. 16, 22, 24, and 44). The mean coupling voltage has been steady at -10.2 ± 0.2 V over the duration of the test. The low coupling voltage magnitude is a result of high keeper current and neutralizer flow rate, selected to maintain neutralizer operation in spot mode throughout ion thruster service life while imposing only modest sacrifices in engine performance. The neutralizer keeper and coupling voltages indicate no neutralizer performance degradation.

Figure 19 shows the neutralizer flow margin, which is the difference between the neutralizer flow set point from the throttle table and the transition flow from spot to plume mode operation, as a function of elapsed test duration for multiple beam currents. Spot mode is characterized by low voltage and current oscillations, while plume mode is described by large fluctuations that can lead to reduced emitter life. Following the NSTAR criterion, plume mode operation is reached when peak-to-peak neutralizer keeper voltage oscillations exceed ± 5 V. As Figure 19 illustrates, there is considerable flow margin at the full-power condition. Transition flow margin has decreased for all beam current conditions over the test duration. The least neutralizer flow margin exists for the low-beam current operating conditions where after 15,000 h of operation no margin is available (–0.4 A margin for 1 A beam current). Motivated by the EM neutralizer low flow margin at beginning-of-life, the neutralizer keeper gap on the NEXT PM thruster design is larger than for EM thrusters resulting in double the beginning of life flow margin at low-power at the modest expense of ~ 1 V increase in the magnitude of the coupling voltage (Ref. 9). The beginning-of-life flow margins for the first NEXT PM thruster are shown in Figure 19. With similar degradation, the

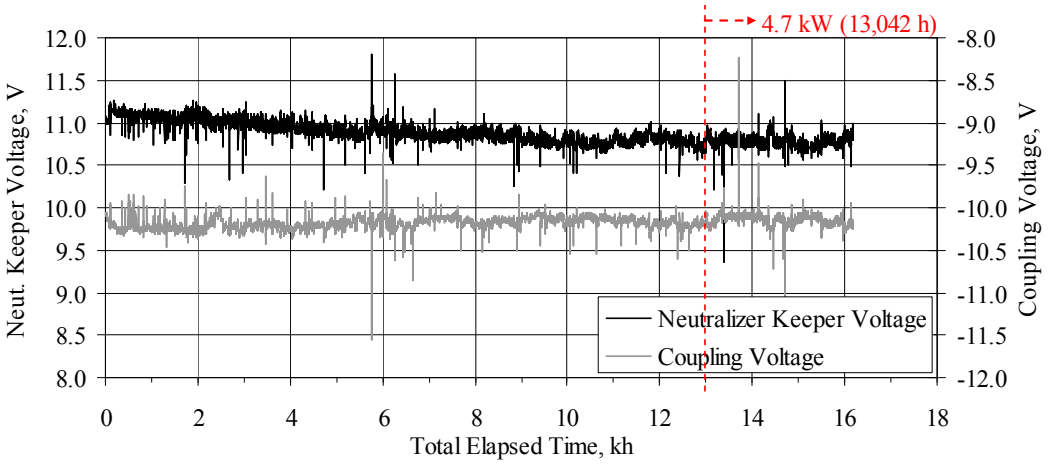

Figure 18.—Full-power and 4.7 kW neutralizer keeper voltage and coupling voltage runtime data.

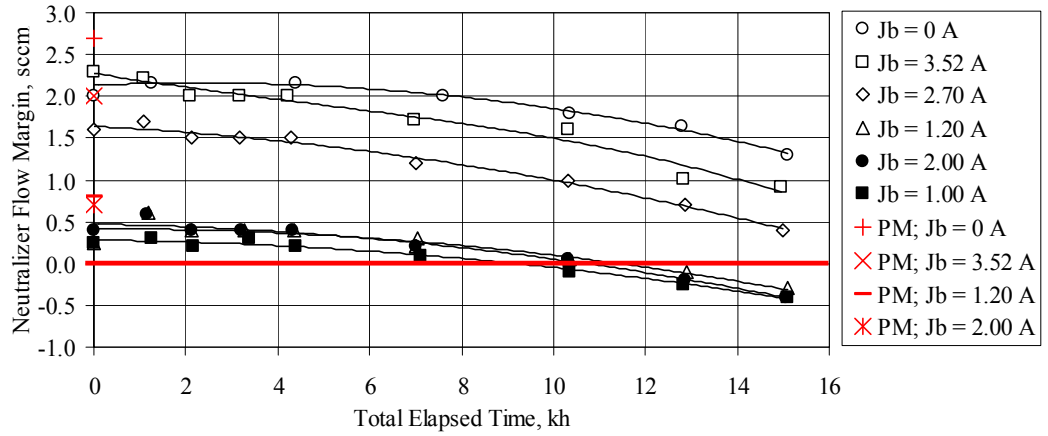

Figure 19.—Neutralizer flow margin, between set flow and transition flow, as a function of time for various beam currents (Ref. 9).

PM thruster would still have 0.10 sccm neutralizer flow margin at the low power operating points of 1.20 A beam currents after 15,000 h of operation. The loss of neutralizer flow margin is however one of the few areas of concern for the NEXT LDT and is being investigated. First, a better understanding of the fundamental cause for the degradation is underway via a neutralizer modeling effort whose goal is to predict orifice erosion geometry as a function of time (for given operating conditions) as well as neutralizer performance including flow margin for those geometries. Secondly, parametric investigations during neutralizer characterizations are being obtained to determine the best method of addressing the observed degradation (i.e., neutralizer flow increase, neutralizer keeper current increase, or a combination of both). Neutralizer flow margin at low power can be increased by small changes in the keeper current (Ref. 51). This approach was implemented for thrusters on the Dawn spacecraft (Ref. 36). The neutralizer investigation results will be incorporated in an updated NEXT throttle table that also takes advantage of the improved PM ion optics performance.

Neutralizer ignitions, 155 to date, have durations typically less than 4 min as shown in Figure 20. The longest duration occurred following an extended thruster downtime for cryo-pump repairs, 5.5 min. The constant neutralizer ignition durations, even after facility regeneration, offers additional evidence to support the role of the graphite discharge cathode keeper in the observed increasing discharge cathode post-regeneration ignitions. The neutralizer cathode assembly (NCA) utilizes a metal keeper electrode that does not absorb moisture as effectively as graphite.

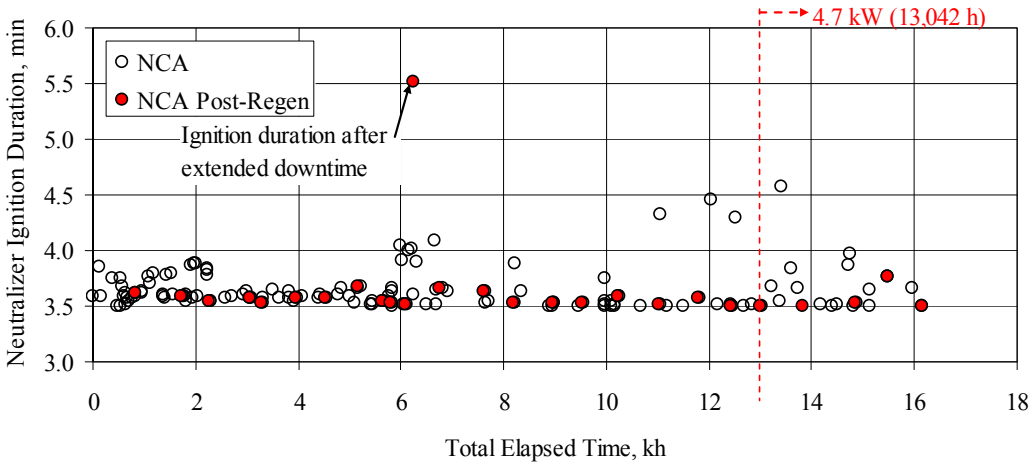

Figure 20.—Thruster neutralizer cathode ignition data as a function of time.

Ion Optics

Beam power supply and accelerator voltages are set to 1800 and –210 V, respectively, during wear test at the full-power point and 1180 and –200 V, respectively, at the 4.7 kW input power operating condition. Accelerator current and wall-mounted facility ion gauge pressure data are plotted as a function of time in Figure 21. As expected, increases in facility pressure cause corresponding increases in accelerator current due to the increased background pressure resulting in higher charge-exchange ion production. Beginning-of-life accelerator currents decreased by 1.5 mA at full-power during the first 100 h of operation, the cause of which is threefold. First, from test start to 49 h, the vacuum facility had only 9 of the 10 cryo-pumps operating resulting in a higher background pressure accounting for 0.5 mA of the 1.5 mA decrease observed. Second, at 94 h, the neutralizer flow was reduced to increase propellant utilization efficiency causing a lower background pressure accounting for 0.3 mA of the 1.5 mA decrease observed. Finally, the thruster ion optics experienced a "burn in" period that is typical to ion thrusters. In NEXT ion thrusters operating at full-power, this burn in is primarily due to enlargement of accelerator grid apertures at large ion optics' radii where the ion current density is low enough to cause direct crossover impingement (Ref. 16 and 21).

Shifts in the facility pressure and accelerator current runtime data after beginning-of-test are due to changes in facility configuration, i.e., the number of operational cryo-pumps, or the effectiveness of cryo-pump(s). Failure of cryo-pumps during extended wear testing is expected over the course of the test based upon the NSTAR ELT experience and repair of failed cryo-pumps requires removal from the facility (Ref. 23). The increase of 0.7 mA at ~1,900 h was due to change in facility operation from 10 to 9 pumps, with the nonoperating pump located near the thruster. 9-pump operation was maintained until ~6,300 h when 10-pump operation resumed and the accelerator current and pressure dropped accordingly. At ~6,600 h a cryo-pump at the far end of the facility was turned off, but there was no observed change in accelerator current. From 6,900 h until the 9,500 h, 8 cryo-pumps were operated, with the two nonoperating cryo-pumps located at the far end of the tank from the thruster. The accelerator currents for 8-pump operation with both non-operating cryos located far from the thruster and 9-pump operation with the nonoperating cryo located near the thruster are within 0.2 mA. The indicated dip in facility pressure from 4,000 to 4,500 h was a measurement error due to contamination of the ion gauge filament that was not degassed periodically, as recommended by the manufacturer, until after this time. Since 9,500 h, 9 cryo-pumps have been operated with the non-operating pump located at the far end of the vacuum tank from the thruster. A step-increase in runtime accelerator current is seen following throttling to the new operating point after 13,042 h of operation. The cause for the increase is more divergent beamlets in the high-density beam regions resulting from the decreased total voltage. "Spikes" in accelerator current are

due to engine shutdowns, restarts, recycles, and facility pressure spikes as the need for a facility regeneration is approached (Refs. 32 and 52).

Figure 22 shows the accelerator current runtime data and the accelerator currents for each of the performance operating conditions as a function of time. An initial decrease in accelerator current is observed at the beginning of the test due to increased pumping speed when transitioning from 9 to 10 cryo-pumps, the neutralizer flowrate decrease, and the outer radii accelerator grid aperture enlargement. After the beginning of the test, the accelerator current trends have been dominated by changes in the facility background pressure. In contrast, NSTAR ion thruster accelerator currents in wear tests have generally started higher than nominal requiring up to 1,500 h to decrease to nominal values resulting in greater variability in performance and erosion (Refs. 22 and 44). The accelerator current for the NSTAR thruster on DS1 was ~25 percent less in space than the NSTAR data obtained during pre-flight measurements in a test facility operating with a background pressure level of 3.5×10^{-6} torr (Refs. 3, 23, and 44). Because the NEXT LDT is operating at comparable yet slightly higher operating background pressures, it is expected that the NEXT in space accelerator current would be reduced by ≥25 percent compared to those measured in this test facility.

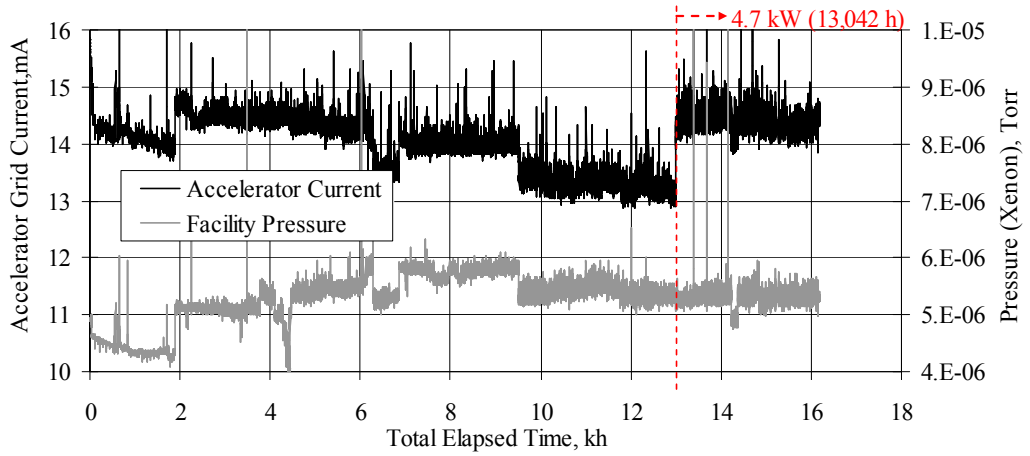

Figure 21.—Accelerator grid current and background facility pressure (wall ion gauge) runtime data.

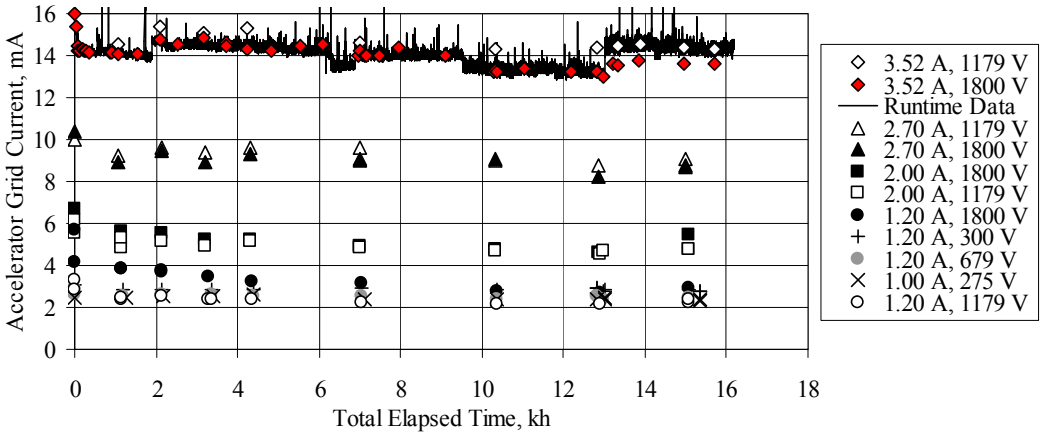

Figure 22.—Thruster accelerator grid current data as a function of time.

Electron backstreaming margins, perveance margins, and screen grid ion transparencies throughout the wear test are plotted for each operating condition in Figure 23 to Figure 25, respectively. Electron backstreaming limit is the highest accelerator voltage, lowest in magnitude, which will prevent beam plasma electrons from backstreaming through the ion optics. Electron backstreaming limits are determined by lowering the magnitude of the accelerator grid voltage until the indicated beam power supply current increases by 1 mA due to backstreaming electrons. The electron backstreaming margin is then the difference between the setpoint and the limit. Impingement-limited total voltage is a measure of the ion optics' current extraction capability, and therefore a measure of its perveance. Perveance limits are determined from plots of accelerator current as a function of total voltage where the slope is –0.02 mA/V, the NSTAR criterion. The total voltage is defined as the sum of the beam power supply voltage and the absolute value of the accelerator grid voltage. Screen grid ion transparencies are calculated as described in Reference 53.

Electron backstreaming margin has been relatively constant for all operating conditions over the entire test duration, however a slightly increasing trend is discernable. At full-power, the electron backstreaming margin has improved by ~5 V since BOL. The backstreaming limit has been observed to decrease following perveance measurements indicating the cause of the improved margin may be the result of sputtered deposition on the accelerator cusps, which is removed when the beamlets are defocused during perveance measurements. Electron backstreaming margins have remained constant for all operating conditions investigated since throttling the thruster to 4.7 kW input power. Perveance margins have been nominal, within measurement error, over the duration of the test indicating no substantial change in accelerator aperture cusps or operating ion optics' grid-gap. A modest decrease, approximately 1 percentage point, in screen grid ion transparency is observed over the duration of the test likely due to the increasing sheath thickness on the screen grid caused by the increasing discharge voltage, in Figure 25. Changes in electron backstreaming limit, perveance limit, and screen grid ion transparencies are not significant enough to degrade the ion optics' performance and are less than or equal to those exhibited by the NSTAR ion optics during the 8,200 h wear test and NSTAR ELT (Refs. 22 and 25). Electron backstreaming and perveance margins are equal to or greater than their pre-test values with the most recent values for the full-power test condition are ~40 and 1150 V, respectively. With such large electron backstreaming margin, there is the opportunity to reduce the full-power accelerator voltage magnitude, which was based upon EM ion optics' performance, in order to reduce accelerator erosion.

Perveance data, shown in Figure 24, has been constant at all operating conditions investigated within the error of the measurement with one exception occurring for the 1.00 A beam current operating condition. The 1.00 A case perveance limit appears to increase by ~100 V for data taken between 1,000 to 5,000 h. This apparent increase is a result of the dependence of perveance on the ratio of beam-to-total voltage or R ratio. During the beginning-of-test characterization the accelerator grid voltage was –400 V. Subsequent operation at 1.00 A beam current was conducted with an accelerator grid voltage of –500 V as

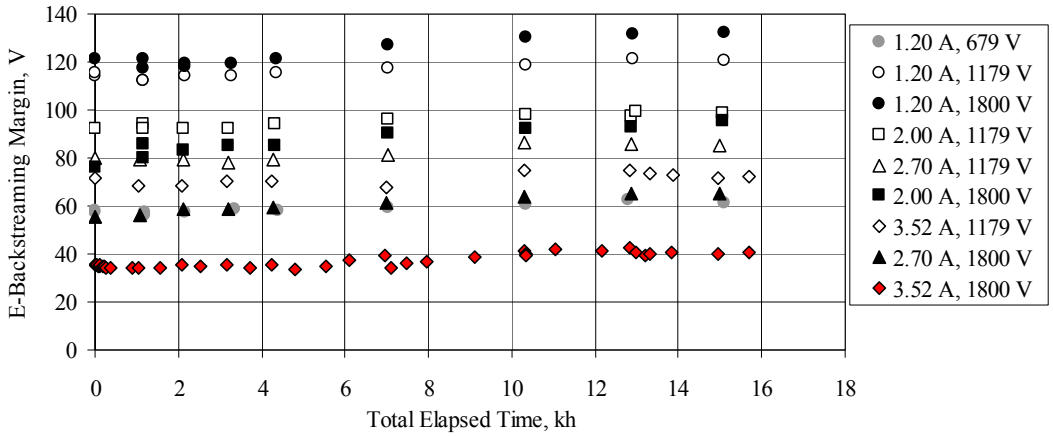

Figure 23.—Thruster ion optics' electron backstreaming limit data as a function of time.

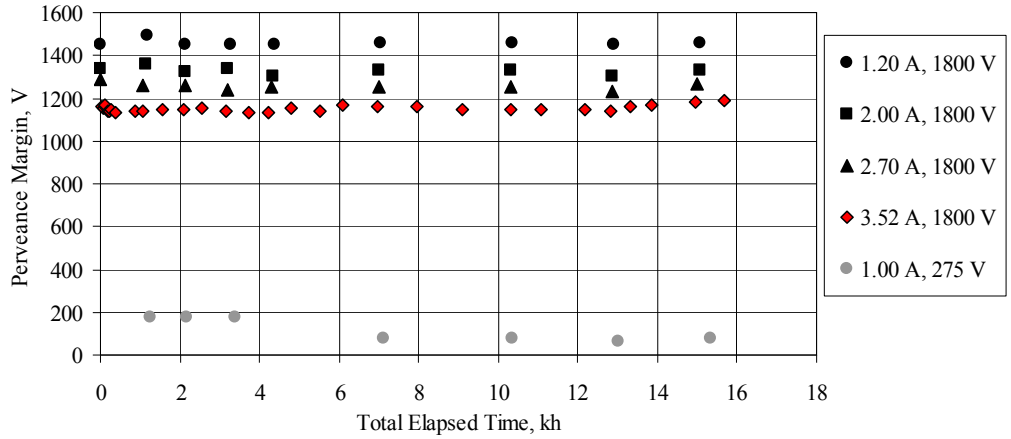

Figure 24.—Thruster ion optics' impingement-limited total voltage data as a function of time.

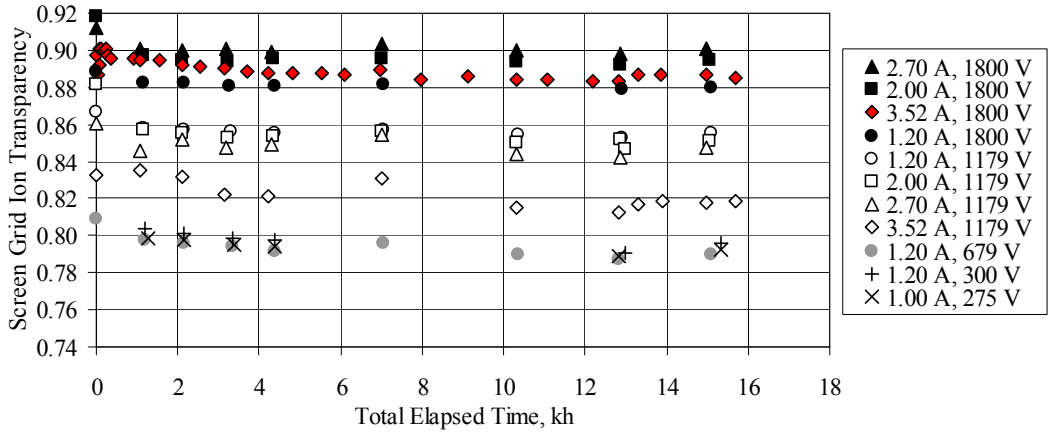

Figure 25.—Thruster ion optics' screen grid ion transparency data as a function of time.

indicated in the NEXT throttling table. During the LDT, sufficient electron backstreaming margin was available with the PM ion optics to warrant a revisiting of the accelerator voltage value in the NEXT throttle table. A reduction of the accelerator voltage would reduce accelerator grid erosion at this low power operating condition. Perveance data taken after 6,000 h of operation was obtained with an accelerator voltage of –400 V.

A recycle event is a series of power supply commands that follows a high-current arc between ion optic grids to prevent instigation of subsequent arcs during which the following occur sequentially: the grid potentials are commanded to zero, the discharge current is reduced, the accelerator grid potential is reapplied, the screen grid potential is reapplied, and finally the discharge current is increased back to the nominal value. The LDT recycle rate, averaged over 15 h, and the total number thruster recycles as a function of time are plotted in Figure 26. The recycle data have been corrected by removing recycles occurring during performance testing where numerous recycles can be induced, such as during perveance measurements. The recycle rate has been 1 to 3 recycles per hour over the majority of the test duration. One noticeable exception occurs at ~6,300 h where as many as 9 recycles per hour were observed for a short duration. This increase occurred following the extended thruster downtime for facility repairs after ~19 μm of back-sputtered carbon had accumulated on the thruster optics. During multiple facility regenerations at this time, absorption of water by the thin carbon films lead to spalling, which is visible on the neutralizer enclosure and front mask and was likely the cause of the increased recycle rate observed (Refs. 54 to 56).

The recycle rate rose abruptly once the thruster was throttled to the new operating condition. This was unexpected because the 4.7 kW operating point has a lower total voltage than the full-input-power condition. It is speculated that the high recycle rate was a result of carbon deposition on the ion optics that was being removed by the more divergent beamlets at the new operating condition. That it took ~1,000 h to return to the nominal recycle rate is surprising, but erosion images taken of the accelerator grid apertures confirm removal of carbon deposits inside the apertures and on the downstream surface of the grid.

The total number of recycles for the NEXT LDT and two NSTAR wear tests are plotted as a function of propellant throughput in Figure 27 (Refs. 22 and 25). NEXT is expected to demonstrate a slightly higher recycle rate due to its larger beam extraction area and higher inter-grid electric field at full-power that are 1.6X and 1.5X that of the NSTAR thruster at full-power, respectively. Figure 27 shows that when plotted against propellant throughput, removing the beam extraction area dependence, the recycle rate of the NEXT LDT at full-power is similar to the NSTAR wear tests. This is somewhat unexpected since the total recycles as a function of propellant throughput plot does not account for the increased NEXT inter-grid electric field. The NSTAR ELT was throttled to lower power operating conditions during the test, which resulted in inter-grid electric fields lower than the NSTAR full-power condition (Refs. 23 and 25). Additionally, the NEXT LDT backsputtered film thickness deposited on the thruster optics is several multiples greater than that of the NSTAR ELT and 2,000 h wear test, respectively. However, the NEXT PM ion optics' operating grid-gap has been measured to be slightly larger than the NSTAR thruster, which may help explain the similar recycle rates (Refs. 39, 57, and 58). Spalling of thin films will artificially increase the recycle rate compared to in space operation. The recycle rate in space is expected to be dramatically reduced. For example, the DS1 ion engine had only 7 recycles per hundred hours during its first operational segment (Ref. 59).

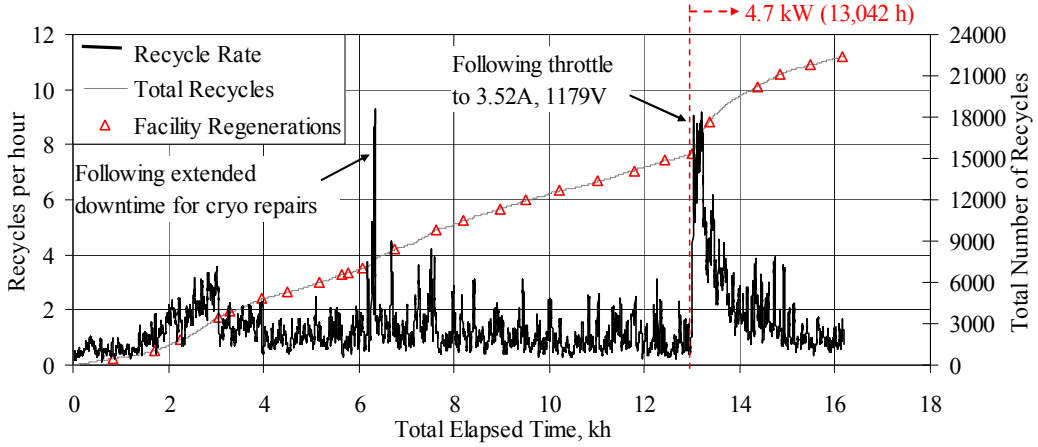

Figure 26.—Thruster recycle rate and total number of recycles runtime data as a function of time.

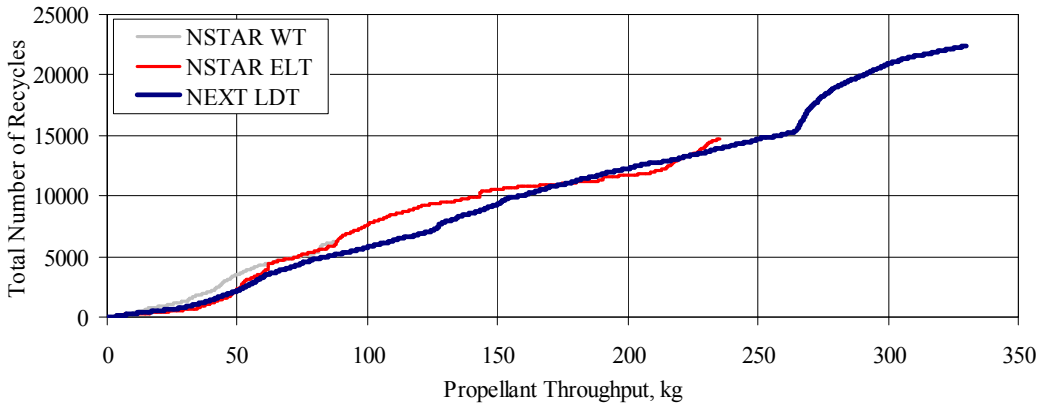

Figure 27.—Total number of recycles as a function of propellant throughput for the NEXT LDT, NSTAR ELT, and NSTAR 8,200 h wear test (Refs. 22 and 23).

Beginning-of-Life and Post-300 kg Performance Comparison

A summary of key thruster performance parameters comparing beginning-of-life performance to performance after processing 300 kg of Xe is shown in Table 3. The table identifies the thruster operating condition by the unique combination of beam current and beam power supply voltage. Performance parameters are listed with the relevant associated uncertainties including: thruster input power, specific impulse, thrust efficiency, and discharge propellant utilization efficiency. Note that the pretest characterization testing was performed with a higher neutralizer flow rate for many operating conditions. An intentional decrease in neutralizer flow following the beginning-of-life characterization was made to improve overall propellant utilization efficiency resulting in increases in specific impulse and thrust efficiency. The neutralizer flow rate has been shown in Table 3 to highlight the different values for the operating conditions at the beginning of life compared to performance after 300 kg. All other input operating parameters for a given beam current and beam power supply voltage are identified in Table A.1.

TABLE 3.—NEXT LDT PERFORMANCE COMPARISON OF BEGINNING-OF-LIFE (SHADED) AND AFTER 300 kg Xe PROCESSED FOR OPERATING CONDITIONS SPANNING THE NEXT THROTTLE TABLE
[Full-power condition is in bold.]

J_B, A	V_B, V	P_{IN}, kW	Thrust, mN	Thrust uncertainty, mN	Isp, sec	Isp uncertainty, sec	Thrust efficiency	Thrust efficiency. uncertainty	Discharge. propellant efficiency[a]	m_N, sccm
3.52	**1800**	**6.83**	**237**	**± 3**	**4090**	**± 70**	**0.695**	**± 0.017**	**0.889**	**5.16**
3.52	**1800**	**6.86**	**237**	**± 3**	**4170**	**± 70**	**0.706**	**± 0.017**	**0.889**	**4.01**
3.52	1180	4.67	192	± 2	3320	± 60	0.666	± 0.017	0.889	5.16
3.52	1180	4.70	192	± 2	3380	± 60	0.676	± 0.017	0.889	4.01
2.70	1800	5.27	182	± 2	4020	± 70	0.680	± 0.017	0.889	4.75
2.70	1800	5.28	182	± 2	4130	± 70	0.696	± 0.017	0.889	3.50
2.70	1180	3.61	147	± 2	3260	± 60	0.652	± 0.017	0.890	4.75
2.70	1180	3.63	147	± 2	3350	± 60	0.666	± 0.017	0.889	3.50
2.00	1800	3.96	134	± 2	4060	± 70	0.673	± 0.017	0.930	4.41
2.00	1800	3.96	134	± 2	4230	± 70	0.701	± 0.017	0.928	3.00
2.00	1180	2.72	108	± 1	3290	± 60	0.642	± 0.017	0.930	4.41
2.00	1180	2.73	108	± 1	3420	± 60	0.666	± 0.017	0.928	3.00
1.20	1800	2.43	80	± 1.0	3800	± 70	0.615	± 0.017	0.928	4.01
1.20	1800	2.42	80	± 1.0	3890	± 70	0.632	± 0.017	0.927	3.50
1.20	1180	1.70	65	± 0.8	3090	± 50	0.581	± 0.017	0.931	4.01
1.20	1180	1.69	65	± 0.8	3180	± 50	0.602	± 0.017	0.927	3.30
1.20	679	1.12	49	± 0.6	2340	± 40	0.504	± 0.017	0.930	4.01
1.20	679	1.10	49	± 0.6	2380	± 40	0.521	± 0.017	0.926	3.50
1.20	300	0.648	32	± 0.4	1510	± 30	0.365	± 0.017	0.928	4.01
1.20	300	0.651	32	± 0.4	1540	± 30	0.371	± 0.017	0.926	3.50
1.00	275	0.518	26	± 0.3	1400	± 20	0.340	± 0.017	0.872	3.01
1.00	275	0.520	26	± 0.3	1360	± 20	0.329	± 0.017	0.868	3.50

[a]Corrected for ingested mass flow.

The summary of thruster performance shows negligible performance degradation after 300 kg of Xe processed. Calculated thrust has remained constant while thruster input power has increased by as much as 30 W due to increase discharge losses due to aperture erosion. Discharge propellant utilization efficiency has slightly decreased by less than 0.5 percentage points due to increased neutral loss rate driven by ion optics' aperture erosion processes. Specific impulse and thrust efficiency values are nearly constant, within the measurement uncertainty, with improvements in both for most operating conditions after 300 kg of Xe processed due to the decreased neutral flow rate following the pretest characterization. For conditions of low beam current, the neutralizer flow rate has increased for the most recent

performance characterizations. This increase is required to maintain spot-mode operation, i.e., lower erosion, as a result of the decreasing neutralizer spot-to-plume mode transition flow margin described previously.

Conclusion

The results of the NEXT Long-Duration Test (LDT) as of June 25, 2008, are presented. The NEXT EM3 thruster has accumulated 16,550 h of operation, processed 337 kg of Xe, and demonstrated a total impulse of 13.3×10^6 N·s. *The NEXT thruster has surpassed the total throughput demonstrated by any ion thruster including the NSTAR flight spare thruster used in the extended life test. The NEXT LDT total impulse is the highest ever demonstrated by an ion thruster.* Thruster performance is characterized periodically over the throttling range of 0.5 to 6.9 kW, with calculated thrust of 26 to 237 mN, respectively. At low and high input power, the thruster specific impulses and thrust efficiencies are 1360, 0.319 and 4170 sec, 0.706, respectively. Overall thruster performance, which includes thrust, input power, specific impulse, and thrust efficiency, has remained constant with no signs of degradation. Impingement-limited total voltages, electron backstreaming limits, and screen grid ion transparencies have been steady to date, with a modest improvement in electron backstreaming margin due to facility effects. Discharge losses have increased by 8 W/A at full-power due to increasing discharge voltage and current, with the latter due to increased neutral loss resulting from accelerator aperture erosion. Neutralizer keeper voltage has slightly decreased by 0.5 V due to orifice channel erosion and coupling voltage has been steady with no indication of performance degradation. Neutralizer transition flow margin has decreased and is being addressed via modeling effort to predict future behavior and a parametric investigation to determine the best mitigation strategy. Comparison of thruster beginning-of-test and post-300 kg performance demonstrates negligible performance degradation. All thruster performance trends indicate that the NEXT thruster will achieve the qualification propellant throughput of 450 kg.

Appendix

TABLE A.1.—NEXT ION THRUSTER THROTTLE TABLE WITH LDT PERFORMANCE OPERATING CONDITIONS SUBSET SHADED
[Full-power wear test condition in bold.]

P_{IN}, kW[a]	J_B, A	V_B, V	V_A, V	m_M, sccm	m_C, sccm	m_N, sccm	J_{NK}, A
6.83	**3.52**	**1800**	**–210**	**49.6**	**4.87**	**4.01**	**3.00**
6.03	3.52	1570	–210	49.6	4.87	4.01	3.00
5.43	3.52	1400	–210	49.6	4.87	4.01	3.00
4.68	3.52	1180	–200	49.6	4.87	4.01	3.00
6.03	3.10	1800	–210	43.5	4.54	4.01	3.00
5.32	3.10	1570	–210	43.5	4.54	4.01	3.00
4.80	3.10	1400	–210	43.5	4.54	4.01	3.00
4.14	3.10	1180	–200	43.5	4.54	4.01	3.00
5.27	2.70	1800	–210	37.6	4.26	3.50	3.00
4.65	2.70	1570	–210	37.6	4.26	3.50	3.00
4.19	2.70	1400	–210	37.6	4.26	3.50	3.00
3.61	2.70	1180	–200	37.6	4.26	3.50	3.00
3.20	2.70	1020	–175	37.6	4.26	3.50	3.00
4.60	2.35	1800	–210	32.4	4.05	3.50	3.00
4.06	2.35	1570	–210	32.4	4.05	3.50	3.00
3.66	2.35	1400	–210	32.4	4.05	3.50	3.00
3.16	2.35	1180	–200	32.4	4.05	3.50	3.00
2.80	2.35	1020	–175	32.4	4.05	3.50	3.00
4.00	2.00	1800	–210	25.8	3.87	2.50	3.00
3.54	2.00	1570	–210	25.8	3.87	2.50	3.00
3.20	2.00	1400	–210	25.8	3.87	2.50	3.00
2.77	2.00	1180	–200	25.8	3.87	2.50	3.00
2.46	2.00	1020	–175	25.8	3.87	2.50	3.00
3.24	1.60	1800	–210	20.0	3.70	2.75	3.00
2.87	1.60	1570	–210	20.0	3.70	2.75	3.00
2.60	1.60	1400	–210	20.0	3.70	2.75	3.00
2.26	1.60	1180	–200	20.0	3.70	2.75	3.00
2.01	1.60	1020	–175	20.0	3.70	2.75	3.00
2.43	1.20	1800	–210	14.2	3.57	3.00	3.00
2.15	1.20	1570	–210	14.2	3.57	3.00	3.00
1.95	1.20	1400	–210	14.2	3.57	3.00	3.00
1.70	1.20	1180	–200	14.2	3.57	3.00	3.00
1.51	1.20	1020	–175	14.2	3.57	3.00	3.00
1.41	1.20	936	–150	14.2	3.57	3.00	3.00
1.31	1.20	850	–125	14.2	3.57	3.00	3.00
1.11	1.20	679	–115	14.2	3.57	3.00	3.00
1.08	1.20	650	–144	14.2	3.57	3.00	3.00
0.777	1.20	400	–394	14.2	3.57	3.00	3.00
0.656	1.20	300	–525	14.2	3.57	3.00	3.00
0.529	1.00	275	–500	12.3	3.52	3.00	3.00

[a]Nominal values.

References

1. Rayman, M.D., "The Successful Conclusion of the Deep Space 1 Mission: Important Results Without a Flashy Title," Space Technology, vol. 23, pp. 185–196, 2003.
2. Lee, M., et al., "Deep Space 1 Mission and Observation of Comet Borrelly," Deep Space 1 Mission and Observation of Comet Borrelly, 45th IEEE International Midwest Symposium on Circuits and Systems, Tulsa, OK, Aug. 4, 2002.
3. Polk, J.E., et al., "Performance of the NSTAR Ion Propulsion System on the Deep Space One Mission," AIAA–2001–0965, 39th AIAA Aerospace Sciences Meeting and Exhibit Joint Propulsion Conference, Reno, NV, Jan. 8–11, 2001.
4. Oleson, S., et al., "Outer Planet Exploration with Advanced Radioisotope Electric Propulsion," IEPC Paper 2001–0179 and NASA/TM—2002-211314, 27th International Electric Propulsion Conference, Pasadena, CA, Oct. 15–19, 2001.
5. Oleson, S., et al., "Mission Advantages of NEXT: NASA's Evolutionary Xenon Thruster," AIAA–2002–3969, 38th AIAA/ASME/SAE/ASEE Joint Propulsion Conference and Exhibit, Indianapolis, IN, July 7–10, 2002.
6. Cupples, M., et al., "Application of Solar Electric Propulsion to a Comet Surface Sample Return Mission," AIAA–2004–3804, 40th AIAA/ASME/SAE/ASEE Joint Propulsion Conference and Exhibit, Fort Lauderdale, FL, Jul. 11–14, 2004.
7. Benson, S.W., et al., "NEXT Ion Propulsion System Configurations and Performance for Saturn System Exploration," AIAA–2007–5230, 43rd AIAA/ASME/SAE/ASEE Joint Propulsion Conference and Exhibit, Cincinnati, OH, Jul. 8–11, 2007.
8. Oh, D., et al., "Deep Space Mission Applications for NEXT: NASA's Evolutionary Xenon Thruster," AIAA–2004–3806, 40th AIAA/ASME/SAE/ASEE Joint Propulsion Conference and Exhibit, Fort Lauderdale, FL, Jul. 11–14, 2004.
9. Herman, D.A., et al., "Performance Evaluation of the Prototype-Model NEXT Ion Thruster," AIAA–2007–5212, 43rd AIAA/ASME/SAE/ASEE Joint Propulsion Conference and Exhibit, Cincinnati, OH, Jul. 8–11, 2007.
10. Pinero, L.R., et al., "Integration and Qualification of the NEXT Power Processing Unit," AIAA–2007–5214, 43rd AIAA/ASME/SAE/ASEE Joint Propulsion Conference and Exhibit, Cincinnati, OH, Jul. 8–11, 2007.
11. Patterson, M.J. and Benson, S.W., "NEXT Ion Propulsion System Development Status and Capabilities," Conference Proceedings and NASA/TM—2008-214988, 2007 NASA Science Technology Conference, College Park, MD, Jun.19–21, 2007.
12. Snyder, J.S., et al., "Vibration Test of a Breadboard Gimbal for the NEXT Ion Engine," AIAA–2006–4665, 42nd AIAA/ASME/SAE/ASEE Joint Propulsion Conference and Exhibit, Sacramento, CA, Jul. 9–12, 2006.
13. Aadland, R. S., et al., "Development Status of the NEXT Propellant Management System," AIAA–2004–3974, 40th AIAA/ASME/SAE/ASEE Joint Propulsion Conference and Exhibit, Fort Lauderdale, FL, Jul. 11–14, 2004.
14. Hoskins, W.A., et al., "Development of a Prototype Model Ion Thruster for the NEXT System," AIAA–2004–4111, 40th AIAA/ASME/SAE/ASEE Joint Propulsion Conference and Exhibit, Fort Lauderdale, FL, Jul. 11–14, 2004.
15. Monheiser, J., et al., "Development of a Ground Based Digital Control Interface Unit (DCIU) for the NEXT Propulsion System," AIAA–2004–4112, 40th AIAA/ASME/SAE/ASEE Joint Propulsion Conference and Exhibit, Fort Lauderdale, FL, Jul. 11–14, 2004.
16. Soulas, G.C., et al., "NEXT Ion Engine 2000 Hour Wear Test Results," AIAA–2004–3791, 40th AIAA/ASME/ SAE/ASEE Joint Propulsion Conference and Exhibit, Fort Lauderdale, FL, Jul. 11–14, 2004.

17. Van Noord, J.L. and Williams, G.J., "Lifetime Assessment of the NEXT Ion Thruster," AIAA–2007–5274, 43rd AIAA/ASME/SAE/ASEE Joint Propulsion Conference and Exhibit, Cincinnati, OH, Jul. 8–11, 2007.
18. Herman, D.A., et al., "NASA's Evolutionary Xenon Thruster (NEXT) Component Verification Testing," AIAA–2008–4812, 44th AIAA/ASME/SAE/ASEE Joint Propulsion Conference and Exhibit, Hartford, CT, Jul. 21–23, 2008.
19. Van Noord, J.L. and Herman, D.A., "Application of the NEXT Ion Thruster Lifetime Assessment to Thruster Throttling," AIAA–2008–4526, 44th AIAA/ASME/SAE/ASEE Joint Propulsion Conference and Exhibit, Hartford, CT, Jul. 21–23, 2008.
20. Kamhawi, H., et al., "NEXT Ion Engine 2000 hour Wear Test Plume and Erosion Results," AIAA–2004–3792, 40th AIAA/ASME/SAE/ASEE Joint Propulsion Conference and Exhibit, Fort Lauderdale, FL, Jul. 11–14, 2004.
21. Malone, S. P., "Investigation of NEXT Ion Optics Erosion Processes using Computational Modeling," 2005–0356DV, NASA Glenn Research Center, Cleveland, OH, Oct. 20, 2005.
22. Polk, J.E., et al., "An Overview of the Results from an 8200 Hour Wear Test of the NSTAR Ion Thruster," AIAA–1999–2446, 35th AIAA/ASME/SAE/ASEE Joint Propulsion Conference and Exhibit, Los Angeles, CA, Jun. 20–24, 1999.
23. Sengupta, A., et al., "The 30,000-Hour Extended-Life Test of the Deep Space 1 Flight Spare Ion Thruster," NASA/TP—2004-213391, The Jet Propulsion Laboratory and NASA Glenn Research Center, Pasadena, March, 2005.
24. Polk, J.E., et al., "A 1000 Hour Wear Test of the NASA NSTAR Ion Thruster," AIAA–1996–2784, 32nd AIAA/ASME /SAE/ASEE Joint Propulsion Conference and Exhibit, Lake Buena Vista, FL, Jul. 1–3, 1996.
25. Sengupta, A., et al., "An Overview of the Results from the 30,000 Hr Life Test of Deep Space 1 Flight Spare Engine," AIAA–2004–3608, 40th AIAA/ASME/SAE/ASEE Joint Propulsion Conference and Exhibit, Fort Lauderdale, FL, Jul. 11–14, 2004.
26. Doerner, R.P., et al., "Sputtering Yield Measurements during Low Energy Xenon Plasma Bombardment," Journal of Applied Physics, vol. 93, no. 9, pp. 5816–5823, May 1, 2003.
27. Sovey, J., et al., "Retention of Sputtered Molybdenum on Ion Engine Discharge Chamber Surfaces," IEPC Paper 2001–086, 27th International Electric Propulsion Conference, Pasadena, CA, Oct. 15–19, 2001.
28. Patterson, M.J. and Benson, S.W., "NEXT Ion Propulsion System Development Status and Performance," AIAA–2007–5199, 43rd AIAA/ASME/SAE/ASEE Joint Propulsion Conference and Exhibit, Cincinnati, OH, Jul. 8–11, 2007.
29. Soulas, G.C. and Patterson, M.J., "NEXT Ion Thruster Performance Dispersion Analyses," AIAA–2007–5213, 43rd AIAA/ASME/SAE/ASEE Joint Propulsion Conference and Exhibit, Cincinnati, OH, Jul. 8–11, 2007.
30. Soulas, G. C., et al., "Performance Evaluation of the NEXT Ion Engine," AIAA–2003–5278, 39th AIAA/ASME/SAE/ASEE Joint Propulsion Conference and Exhibit, Huntsville, AL, Jul. 20–23, 2003.
31. Patterson, M.J., et al., "NEXT: NASA's Evolutionary Xenon Thruster," AIAA–2002–3832, 38th AIAA/ASME/SAE/ASEE Joint Propulsion Conference and Exhibit, Indianapolis, IN, Jul. 7–10, 2002.
32. Frandina, M.M., et al., "Status of the NEXT Ion Thruster Long Duration Test," AIAA–2005–4065, 41st AIAA/ASME/SAE/ASEE Joint Propulsion Conference and Exhibit, Tucson, AZ, Jul. 10–13, 2005.
33. Kamhawi, H., et al., "NEXT Ion Engine 2000 hour Wear Test Plume and Erosion Results," AIAA–2004–3792, 40th AIAA/ASME/SAE/ASEE Joint Propulsion Conference and Exhibit, Fort Lauderdale, FL, Jul. 11–14, 2004.

34. Hickman, T.A., et al., "Overview of the Diagnostics for the NEXT Long Duration Test," AIAA–2005–4064, 41st AIAA/ASME/SAE/ASEE Joint Propulsion Conference and Exhibit, Tucson, AZ, Jul. 10–13, 2005.
35. Snyder, J. S., et al., "Single-String Integration Test Measurements of the NEXT Ion Engine Plume," AIAA–2004–3790 and NASA/TM—2005-213196, 40th AIAA/ASME/SAE/ASEE Joint Propulsion Conference and Exhibit, Fort Lauderdale, FL, Jul. 11–14, 2004.
36. Brophy, J.R., et al., "The Ion Propulsion System for Dawn," AIAA–2003–4542, 39th AIAA/ASME/SAE/ASEE Joint Propulsion Conference and Exhibit, Huntsville, AL, July 20–23, 2003.
37. Brophy, J.R., et al., "Status of the Dawn Ion Propulsion System," AIAA–2004–3433, 40th AIAA/ASME/SAE/ASEE Joint Propulsion Conference and Exhibit, Fort Lauderdale, FL, Jul. 11–14, 2004.
38. Myers, R.M., "Proceedings of the Nuclear Electric Propulsion Workshop, Volume 1: Introductory Material and Thruster Concepts, Section: "MPD Thruster Technology"," JPL D–9512 vol. 1, Jun. 19–22, 1990.
39. Herman, D.A., et al., "NEXT Long-Duration Test Plume and Wear Characteristics after 16,550 h of Operation and 337 kg of Xenon Processed," AIAA–2008–4919, 44th AIAA/ASME/SAE/ASEE Joint Propulsion Conference and Exhibit, Hartford, CT, Jul. 21–23, 2008.
40. Van Noord, J.L., "Lifetime Assessment of the NEXT Ion Thruster," AIAA–2007–5274, 43rd AIAA/ASME/SAE/ ASEE Joint Propulsion Conference and Exhibit, Cincinnati, OH, Jul. 8–11, 2007.
41. Patterson, M.J., et al., "Performance of the NASA 30 cm Ion thruster," IEPC Paper 93–108, 23rd International Electric Propulsion Conference, Seattle, WA, Sep. 13–16, 1993.
42. Sovey, J.S., "Improved Ion Containment using a Ring-Cusp Ion Thruster," Journal of Spacecraft and Rockets, vol. 21, no. 5, pp. 488–495, Sep.–Oct. 1984.
43. Stueber, T. and Soulas, G.C., "Electrostatic Ion Thruster Diagnostic Uncertainty Analysis," NASA/TP—2007-214665, (to be published).
44. Anderson, J. R., et al., "Results of an On-going Long Duration Ground Test of the DS1 Flight Spare Ion Engine," AIAA–1999–2857, 35th AIAA/ASME/SAE/ASEE Joint Propulsion Conference and Exhibit, Los Angeles, CA, Jun. 20–24, 1999.
45. Anderson, J.R., et al., "Performance Characteristics of the NSTAR Ion Thruster During an On-Going Long Duration Ground Test," 2000 IEEE Aerospace Conference Proceedings, vol. 4, pp. 123–148, Mar. 2000.
46. Williams, G.J., "High-Power Electric Propulsion (HiPEP) 2,000-Hour Post-Test Report," submitted for publication as NASA/CR, NASA Glenn Research Center, Cleveland, OH, Sep. 2006.
47. Britton, M., et al., "Destructive Analysis of the NEXT 2000-Hour Wear Test Hollow Cathode Assemblies," NASA/TM—2005-213387, NASA Glenn Research Center, Cleveland, OH, Jul. 2005.
48. Williams, G.J., et al., "Results of the 2000 hr Wear Test of the HiPEP Ion Thruster with Pyrolitic Graphite Ion Optics," AIAA–2006–4668, 4nnd AIAA/ASME/SAE/ASEE Joint Propulsion Conference and Exhibit, Sacramento, CA, Jul. 9–12, 2006.
49. Herman, D.A., et al., "Status of the NEXT Ion Thruster Long-Duration Test after 10,100 h and 207 kg Demonstrated," AIAA–2007–5272, 43rd AIAA/ASME/SAE/ASEE Joint Propulsion Conference and Exhibit, Cincinnati, OH, Jul. 8–11, 2007.
50. Herman, D.A., et al., "NEXT Long-Duration Test after 11,570 h and 237 kg of Xenon Processed," IEPC–2007–033, 30th International Electric Propulsion Conference, Florence, Italy, Sep. 17–20, 2007.
51. Brophy, J.R., et al., "The DS1 Hyper-Extended Mission," AIAA–2002–3673, 2002.
52. Soulas, G.C., et al., "Status of the NEXT Ion Engine Wear Test," AIAA–2003–4863, 39th AIAA/ASME/SAE/ASEE Joint Propulsion Conference and Exhibit, Huntsville, AL, Jul 20–23, 2003.
53. Soulas, G.C., et al., "Performance of Titanium Optics on a NASA 30 cm Ion Thruster," AIAA–2000–3814, 36th AIAA/ASME/SAE/ASEE Joint Propulsion Conference and Exhibit, Huntsville, AL, Jul. 16–19, 2000.

54. Hanna, J., et al., “Carbon Film Deposition and Flaking Studies in Ion Thruster Environments,” AIAA–2005–3524, 41st AIAA/ASME/SAE/ASEE Joint Propulsion Conference and Exhibit, Tucson, AZ, Jul. 10–13, 2005.
55. Shigeki, T., et al., “Humidity Dependence of Microwear Characteristics of Amorphous Carbon Films on Silicon Substrates,” International Journal on the Science and Technology of Friction, Lubrication, and Wear, vol. 254, pp. 1042–1049, 2003.
56. Klages, C.P., et al., “Deposition and Properties of Carbon-Based Amorphous Protective Coatings,” Surface and Coating Technology, vol. 80, no. 1–2, pp. 121–128, March 1, 1996.
57. Diaz, E. and Soulas, G.C., “Grid Gap Measurement for an NSTAR Ion Thruster,” IEPC–2005–244, 29th International Electric Propulsion Conference, Princeton, NJ, Oct. 31–Nov. 4, 2005.
58. Soulas, G.C. and Frandina, M.M., “Ion Engine Grid Gap Measurements,” AIAA–2004–3961, 40th AIAA/ASME/SAE/ASEE Joint Propulsion Conference and Exhibit, Fort Lauderdale, FL, July 11–14, 2004.
59. Spacedaily.com, “Deep Space Testbed a Growing Success,” www.spacedaily.com/news/deep1-99a.html, January 12, 1999.

REPORT DOCUMENTATION PAGE		Form Approved OMB No. 0704-0188

1. REPORT DATE *(DD-MM-YYYY)*	2. REPORT TYPE	3. DATES COVERED *(From - To)*
01-05-2009	Technical Memorandum	

4. TITLE AND SUBTITLE
Performance Characteristics of the NEXT Long-Duration Test After 16,550 h and 337 kg of Xenon Processed

5a. CONTRACT NUMBER

5b. GRANT NUMBER

5c. PROGRAM ELEMENT NUMBER

6. AUTHOR(S)
Herman, Daniel, A.; Soulas, George, C.; Patterson, Michael, J.

5d. PROJECT NUMBER

5e. TASK NUMBER

5f. WORK UNIT NUMBER
WBS 346620.04.05.03.13

7. PERFORMING ORGANIZATION NAME(S) AND ADDRESS(ES)
National Aeronautics and Space Administration
John H. Glenn Research Center at Lewis Field
Cleveland, Ohio 44135-3191

8. PERFORMING ORGANIZATION REPORT NUMBER
E-16927

9. SPONSORING/MONITORING AGENCY NAME(S) AND ADDRESS(ES)
National Aeronautics and Space Administration
Washington, DC 20546-0001

10. SPONSORING/MONITORS ACRONYM(S)
NASA

11. SPONSORING/MONITORING REPORT NUMBER
NASA/TM-2009-215611; AIAA-2008-4527

12. DISTRIBUTION/AVAILABILITY STATEMENT
Unclassified-Unlimited
Subject Category: 20
Available electronically at http://gltrs.grc.nasa.gov
This publication is available from the NASA Center for AeroSpace Information, 301-621-0390

13. SUPPLEMENTARY NOTES

14. ABSTRACT
The NASA's Evolutionary Xenon Thruster (NEXT) program is developing the next-generation ion propulsion system with significant enhancements beyond the state-of-the-art in ion propulsion to provide future NASA science missions with enhanced mission capabilities at a low total development cost. As part of a comprehensive thruster service life assessment utilizing both testing and analyses, a Long-Duration Test (LDT) was initiated to verify the NEXT propellant throughput capability to a qualification-level of 450 kg, 1.5 times the anticipated throughput requirement of 300 kg from mission analyses conducted utilizing the NEXT propulsion system. The LDT is being conducted with a modified, flight-representative NEXT engineering model ion thruster, designated EM3. As of June 25, 2008, the thruster has accumulated 16,550 h of operation: the first 13,042 h at the thruster full-input-power of 6.9 kW with 3.52 A beam current and 1800 V beam power supply voltage. Operation since 13,042 h, i.e., the most recent 3,508 h, has been at an input power of 4.7 kW with 3.52 A beam current and 1180 V beam power supply voltage. The thruster has processed 337 kg of xenon (Xe) surpassing the NSTAR propellant throughput demonstrated during the extended life testing of the Deep Space 1 flight spare ion thruster. The NEXT LDT has demonstrated a total impulse of 13.3×106 N·s; the highest total impulse ever demonstrated by an ion thruster. Thruster performance tests are conducted periodically over the entire NEXT throttle table with input power ranging 0.5 to 6.9 kW. Thruster performance parameters including thrust, input power, specific impulse, and thruster efficiency have been nominal with little variation to date. This paper presents the performance of the NEXT LDT to date with emphasis on performance variations following throttling of the thruster to the new operating condition and comparison of performance to the NSTAR extended life test.

15. SUBJECT TERMS
Ion engines; Ion optics; Ion propulsion; Electric propulsion; Electrostatic propulsion; Plasma propulsion

16. SECURITY CLASSIFICATION OF:			17. LIMITATION OF ABSTRACT	18. NUMBER OF PAGES	19a. NAME OF RESPONSIBLE PERSON
a. REPORT	b. ABSTRACT	c. THIS PAGE			STI Help Desk (email:help@sti.nasa.gov)
U	U	U	UU	34	19b. TELEPHONE NUMBER *(include area code)* 301-621-0390